

# Charge density waves and bond order waves in a quarter filled extended Hubbard ladder

E. Orignac<sup>1,a</sup> and R. Citro<sup>2</sup>

<sup>1</sup> Laboratoire de Physique Théorique de l'École Normale Supérieure<sup>b</sup>, 24, rue Lhomond, 75231 Paris Cedex 05, France

<sup>2</sup> Dipartimento di Fisica "E.R. Caianiello" and Unità INFM di Salerno, Università di Salerno, Via S. Allende, 84081 Baronissi (Sa), Italy

Received 13 February 2003 / Received in final form 15 May 2003

Published online 3 July 2003 – © EDP Sciences, Società Italiana di Fisica, Springer-Verlag 2003

**Abstract.** We investigate the phase diagram of a quarter filled Hubbard ladder with nearest-neighbor Coulomb repulsion using bosonization and renormalization group approach. Focusing on the strong-repulsion regime, we discuss the effect of an interchain exchange interaction  $J_{\perp}$  and interchain repulsion  $V_{\perp}$  on the possible ground states of the system and charge order configurations. Since the spin excitations always possess a gap, we find competing bond-order wave and charge density wave phases as possible ground states of the ladder model. We discuss the elementary excitations in these various phases and point an analogy between the excitations on some of these phases and those of a Kondo-Heisenberg insulator. We also study the order of the quantum phase transitions between the different ground states of the system. We obtain second order transitions in the Ising or  $SU(2)_2$  universality class or first order transitions. We map the complete phase diagram in the  $J_{\perp} - V_{\perp}$  plane by integrating perturbative renormalization-group equations. Finally, we discuss the effect of doping away from half-filling and the effect of an applied magnetic field.

**PACS.** 71.10.Pm Fermions in reduced dimensions (anyons, composite fermions, Luttinger liquid, etc.) – 71.10.Hf Non-Fermi-liquid ground states, electron phase diagrams and phase transitions in model systems – 71.10.Fd Lattice fermion models (Hubbard model, etc.)

## 1 Introduction

Charge ordering is a general phenomenon in condensed matter physics that has been recently observed in a variety of compounds including rare earth manganites [1,2], quasi-one-dimensional (TMTTF)<sub>2</sub>X conductors [3], cuprate or nickelate materials [4,5]. A very particular form of charge order in these latter materials is the formation of *charge stripes*, that are domain walls between hole rich and hole poor regions. From the theoretical point of view, charge ordering is a crystallization of the electron liquid which occurs when long-range Coulomb repulsion [6] dominates over kinetic energy. In one dimension, charge ordering and more generally metal-insulator transitions can be studied in great details due to the existence of powerful analytical [7–9] and numerical [10] methods. In the case of a one-dimensional system, the simplest model [11] of interacting electrons that allows for charge ordering is the Hubbard model extended with an additional nearest-neighbor Coulomb interaction  $V$ . Studies of the metal insulator transition in one dimension show that charge ordered or Mott insulating states can form at commensurate fillings for sufficiently strong repulsion [12,13]. In relation with organic compounds, the

quarter-filled extended Hubbard model on a single chain has been studied in details [14]. As a first step towards understanding charge ordering and stripe formation in strongly correlated electron models, numerical studies of coupled chain systems at commensurate fillings [15–19] (ladders) have also been performed. Half filled ladder systems are Mott insulators that display a spin gap analogous to the Haldane gap in spin-1 chains [20] when made of an even number of coupled chains. Ladder models are not only of theoretical interest. Quite a few half-filled ladder systems have been synthesized both organic and inorganic and the spin gap behavior has been characterized in great details [21–26]. Away from half-filling and more generally commensurate filling, ladders are expected to be conducting. The persistence of the spin gap away from half-filling has been proposed to give rise to a pairing mechanism and to superconductivity [27]. This suggestion has given rise to intense theoretical studies both analytical [28–31] and numerical [32–36] that confirmed the presence of superconducting correlations at incommensurate fillings. Experimentally, the two-leg ladder compound Sr<sub>14</sub>Cu<sub>24</sub>O<sub>41</sub> [37] can be doped away from half filling and under pressure displays a superconducting transition. Recently, the compound  $\alpha' - \text{NaV}_2\text{O}_5$ , initially identified as an inorganic spin Peierls compound [38], was shown to be a quarter-filled ladder [39–42], that undergoes a transition

<sup>a</sup> e-mail: orignac@lpt.ens.fr

<sup>b</sup> CNRS-UMR8549

at  $T_c = 34$  K corresponding to the formation of a charge ordered state with a zig-zag charge pattern and the opening of a spin gap [43–46]. This has prompted numerical studies of quarter-filled extended Hubbard two-leg ladder systems [47,48] that exhibit the formation of a zig-zag charge ordered state at large repulsion. Interestingly, the charge ordered state of the two-leg ladder at quarter filling presents a spin gap in contrast to the single chain. Analytic studies of insulating states on a two-leg ladder have been mostly confined to the half-filled case [49–52] or to mean field [42,53] approximations and strong coupling expansions [41,54,55] in the quarter-filled case. In the present paper we analyze the phase diagram of the quarter-filled two-leg Hubbard ladder with interchain Coulomb repulsion  $V_\perp$  and exchange coupling  $J_\perp$ , by using bosonization and renormalization group (RG) methods. Focusing on the regime of strong repulsion, we discuss charge orders and the elementary excitations of the insulating phase. Due to the presence of a spin gap, the competing ground states are bond-order wave states (BOW) and charge density wave states (CDW). We analyze the phase transitions between these states using a perturbative renormalization group approach and a mapping of spin excitations to a Majorana fermion theory. The plan of the paper is the following. In Section 2 we introduce the model and discuss the physics of two simple limits, the large on-site repulsion and the large interchain exchange limit. In Section 3 we give the details of the bosonization treatment and of the derivation of the renormalization group (RG) equations. In Section 4 we introduce the order parameters of the insulating phases and describe the charge ordered ground states obtained by the values of the phase fields that minimize the energy. In Section 5 we describe the elementary charge and spin excitations of each ground state and discuss the analogy with Kondo-Heisenberg-Hubbard chain in a particular case. In Section 6 we discuss the nature of the transitions among the various phases in the antisymmetric charge sector and the spin sector. This is partially accomplished by a mapping to a theory of Majorana fermions and by a mapping to an effective quantum Ising model in the limit of strong interchain repulsion. Finally, we discuss the results of the phase diagram obtained by the numerical integration of the RG equations. We also briefly discuss the commensurate-incommensurate transitions produced by the application of a magnetic field or by doping away from quarter-filling.

## 2 Hamiltonian and some simple limits

We consider the quarter-filled extended Hubbard model on a two leg ladder. The Hamiltonian reads:

$$\begin{aligned}
 H = & -t \sum_{i,p,\sigma} (c_{i+1,p,\sigma}^\dagger c_{i,p,\sigma} + c_{i,p,\sigma}^\dagger c_{i+1,p,\sigma}) \\
 & -t_\perp \sum_{i,\sigma} (c_{i,2,\sigma}^\dagger c_{i,1,\sigma} + \text{h.c.}) + U \sum_{i,p} n_{i,p,\uparrow} n_{i,p,\downarrow} \\
 & + V_\parallel \sum_{i,p} n_{i,p} n_{i+1,p} + V_\perp \sum_i n_{i,1} n_{i,2}, \quad (1)
 \end{aligned}$$

where  $n_{i,p,\sigma} = c_{i,p,\sigma}^\dagger c_{i,p,\sigma}$ ,  $n_{i,p} = n_{i,p,\uparrow} + n_{i,p,\downarrow}$ ,  $i$  is the site index,  $p$  the chain index,  $t$  the intrachain hopping,  $t_\perp$  the interchain hopping,  $U$  the on-site repulsion,  $V_\parallel$  the nearest-neighbor repulsion, and  $V_\perp$  the interchain repulsion.

Since we will be focusing on the case of very strongly repulsive interactions, the single-particle interchain hopping term  $t_\perp$  will be irrelevant in this regime. However, it is well known that even when  $t_\perp$  is irrelevant, it generates an interchain exchange term in the Hamiltonian [56,30]. Thus, the Hamiltonian (1) should also include an interchain exchange term,

$$H_{\text{exch.}} = J_\perp \sum_i \mathbf{S}_{i,1} \cdot \mathbf{S}_{i,2}, \quad (2)$$

where  $\mathbf{S}_{i,p} = c_{i,p,\alpha}^\dagger \boldsymbol{\sigma}_{\alpha,\beta} c_{i,p,\beta}$ . In the limit of  $t_\perp \ll U$ ,  $J_\perp$  is estimated to second order perturbation theory in  $t_\perp/U$  as  $J_\perp \sim t_\perp^2/U$ . In the following, we will consider the Hamiltonian (1) completed by the term (2) and neglect altogether the interchain hopping  $t_\perp$ . In fact, another model of interest is the two leg t-J ladder at quarter filling. The Hamiltonian of this model reads:

$$\begin{aligned}
 H = & -t \sum_{i,p,\sigma} \mathcal{P}(c_{i+1,p,\sigma}^\dagger c_{i,p,\sigma} + c_{i,p,\sigma}^\dagger c_{i+1,p,\sigma}) \mathcal{P} \\
 & -t_\perp \sum_{i,\sigma} \mathcal{P}(c_{i,2,\sigma}^\dagger c_{i,1,\sigma} + \text{h.c.}) \mathcal{P} \\
 & + J_\parallel \sum_{i,p} \mathbf{S}_{i,p} \cdot \mathbf{S}_{i,p+1} + V_\parallel \sum_{i,p} n_{i,p} n_{i+1,p} \\
 & + J_\perp \sum_i \mathbf{S}_{i,1} \cdot \mathbf{S}_{i,2} + V_\perp \sum_i n_{i,1} n_{i,2}, \quad (3)
 \end{aligned}$$

where  $\mathcal{P}$  is an operator that projects onto singly occupied states [19,57]. We will thus treat  $J_\perp$  as a parameter independent of  $t, U$  in (1) in order to be able to discuss also results relevant to the two-leg t-J ladder model. In the rest of the present section, we will illustrate two simple limiting cases of the problem defined by the Hamiltonian (1–2) which display insulating charge ordered ground states.

### 2.1 Large on-site repulsion

Let us begin by considering the limit  $U \rightarrow \infty$  in the Hamiltonian (1–2). In this limit, it is not possible to put two fermions on the same site even when they have opposite spins and from the point of view of charge excitations, the system behaves as if it was made of spinless fermions with a Fermi wavevector  $k'_F$  twice the one of the spinful fermions at  $U = 0$  [58]. The original spinful fermions system being quarter-filled, the spinless fermions system is half-filled and its effective Hamiltonian reads:

$$\begin{aligned}
 H = & -t \sum_{i,p} (a_{i+1,p}^\dagger a_{i,p} + a_{i,p}^\dagger a_{i+1,p}) + V_\parallel \sum_{i,p} n_{i,p} n_{i+1,p} \\
 & + V_\perp \sum_i n_{i,1} n_{i,2}, \quad (4)
 \end{aligned}$$

where now  $n_{i,p} = a_{i,p}^\dagger a_{i,p}$ . The bosonization of the Hamiltonian (4) is straightforward. The relevant formulas can be found for instance in reference [9]. We obtain the following bosonized Hamiltonian:

$$\begin{aligned}
 H = & \sum_{r=1,2} \left\{ \int \frac{dx}{2\pi} \left[ uK(\pi\Pi_r)^2 + \frac{u}{K}(\partial_x\phi_r)^2 \right] \right. \\
 & + \frac{2g}{(2\pi a)^2} \int dx \cos 4\phi_r \left. \right\} + \frac{V_\perp a}{\pi^2} \int dx \partial_x \phi_1 \partial_x \phi_2 \\
 & + \frac{V_\perp a}{(\pi a)^2} \int dx \cos 2\phi_1 \cos 2\phi_2, \quad (5)
 \end{aligned}$$

where  $\cos 4\phi_{1,2}$  represent the intrachain Umklapp interactions. Let us first set  $V_\perp = 0$  and consider the case in which the intrachain Umklapp processes are irrelevant. This case corresponds to  $|V_\parallel| < 2t$ . The Hamiltonian (4) has then a Luttinger liquid ground state for  $V_\perp = 0$ , and the renormalized Luttinger exponent  $K^*$  can be obtained from studies of the  $t - V$  model [59] as:

$$K^* = \frac{1}{2 - \frac{2}{\pi} \arccos\left(\frac{V_\parallel}{2t}\right)}. \quad (6)$$

In the Luttinger liquid regime, we can set  $g = 0$  and replace  $K$  by  $K^*$  in the Hamiltonian (5). We now turn on  $V_\perp$  small enough that the previous approximation remains valid. The Hamiltonian (5), is then decoupled by introducing the fields  $\phi_\pm = (\phi_1 \pm \phi_2)/\sqrt{2}$  leading to the following Hamiltonian:

$$\begin{aligned}
 H &= H_+ + H_-, \\
 H_r &= \int \frac{dx}{2\pi} \left[ u_r K_r (\pi\Pi_r)^2 + \frac{u_r}{K_r} (\partial_x \phi_r)^2 \right] \\
 &+ \frac{2V_\perp a}{(2\pi a)^2} \int dx \cos \sqrt{8}\phi_r, \quad (7)
 \end{aligned}$$

where  $r = \pm$  and:

$$\begin{aligned}
 u_r^2 &= u^2 \left( 1 + r \frac{K^* V_\perp a}{\pi u} \right) \\
 K_r^2 &= (K^*)^2 \left( 1 + r \frac{K^* V_\perp a}{\pi u} \right)^{-1}. \quad (8)
 \end{aligned}$$

For  $K_r < 1$ , the term  $\cos \sqrt{8}\phi_r$  is relevant and opens a gap in the charge modes. If  $V_\perp \ll u/a$ , this implies that the gap opens as soon as  $K^* < 1$ , whereas the intrachain Umklapp processes become relevant only for  $K^* = 1/2$ . We thus see that for a wide range of  $0 < V_\parallel < 2t$ , although intrachain repulsion  $V_\parallel$  alone is too weak to open a charge gap by itself, the existence of a nonzero interchain repulsion is sufficient to induce an insulating ground state. This is consistent with the numerical observation of a charge gap state forming for  $V_\parallel > 0$  and  $t_\perp < t$  at large  $U$  in reference [48]. In that insulating state, the charge gap should vary as  $\Delta_{\rho+} \sim u/a(V_\perp a/u)^{1/(2-K^+)}$ .

We note from (6) that  $K^* = 1$  corresponds to  $V_\parallel = 0$ , *i.e.* the Hamiltonian (7) is identical to the bosonized

Hamiltonian of the half-filled 1D Hubbard chain,  $\phi_+$  playing the role of  $\phi_\rho$ , and  $\phi_-$  playing the role of  $\phi_\sigma$ . As a result, although the total charge mode is gapful, the anti-symmetric charge mode remains gapless. This insulating state presents the same  $SU(2) \times SU(2) \sim SO(4)$  symmetry as the Hubbard model. In particular, the gapped charge excitations behave like those of the half-filled Hubbard model and the charge gap is  $\Delta_{\rho+} \sim u/a \exp(-Cu/(V_\perp a))$ .

To determine the long range order that is realized in the ground state, we need to fix the values of  $\langle \phi_{1,2} \rangle$  that minimize the classical ground state energy, *i.e.* require that  $\cos 2\langle \phi_1 \rangle \cos 2\langle \phi_2 \rangle$  is negative. Since the density of the spinless fermions reads:

$$\rho_p(x) = -\frac{1}{\pi} \partial_x \phi_p(x) + \frac{1}{\pi a} \cos(2\phi_p - 2k'_F x), \quad (9)$$

where  $p = 1, 2$  is the chain index, this leads to two out of phase charge density waves of wavevector  $2k'_F = \frac{\pi}{a}$  on chains 1 and 2, *i.e.* a zig-zag charge ordering. This ordering is represented in Figure 1. We note that in reference [48], it was found that the charge ordering was formed for  $U = \infty$  only when  $V_\parallel > 2t$  although a charge gap was obtained for  $V_\parallel > 0$ . The reason for this discrepancy in reference [48] could be the presence of  $t/t_\perp \sim 1$ . Turning to transport properties, from (9) the long wavelength density on chain  $p$  is  $\rho_p(x) = -\frac{1}{\pi} \partial_x \phi_p$ . By considering the topological charge of the sine-Gordon models (7), one easily obtains that a charge solitons carries the electrical charge  $\pm e$ . The a.c. electrical conductivity of this system can be obtained from the form factor expansion [60,61].

When  $V_\parallel > 2t$ , the interchain Umklapp processes become relevant and induce the formation of charge density waves on each chain [62]. The effect of  $V_\perp$  is to lock the respective phases of these charge density waves into a zig-zag pattern. Zig-zag charge ordering is thus ubiquitous in the limit  $U = \infty$ .

## 2.2 Large interchain exchange

In the limit in which  $J_\perp \rightarrow \infty$  in (1-2) or in (3), it is again possible to derive a simplified Hamiltonian in a low-energy subspace. Namely, one can restrict to a subspace in which fermions form spin singlet pairs on the same rung. These pairs can then be treated as hardcore bosons [34] moving on a single chain and carrying a charge  $2e$ . For a quarter filled fermion system, the effective boson system is at half-filling. The effective bosonic Hamiltonian reads:

$$H = -\tilde{t} \sum_i (b_i^\dagger b_{i+1} + \text{h.c.}) + \tilde{V} \sum_i n_i n_{i+1}, \quad (10)$$

where  $b_i = \sum_\sigma \sigma c_{i,1,\sigma} c_{i,2,-\sigma}$ , annihilates a singlet pair on site  $i$ . In the limit  $J_\perp \gg t$ , the coefficients  $\tilde{t}, \tilde{V}$  can be obtained from second order perturbation theory as  $\tilde{t} = t^2/J_\perp$ ,  $\tilde{V} = 2t^2/J_\perp + V_\parallel$ . The Hamiltonian (10) is solved exactly by the Bethe ansatz [62], and its spectrum has a gap for  $V_\parallel > 0$ . A bosonization description [62-64] of the

low energy excitations of this system gives:

$$H = \int \frac{dx}{2\pi} \left[ uK(\pi\Pi_b)^2 + \frac{u}{K}(\partial_x\phi_b)^2 \right] - \frac{2\Delta}{(2\pi a)^2} \int dx \cos 4\phi_b, \quad (11)$$

where the mode  $\phi_b$  describes the charge excitations of the hardcore boson system. The electrical charge density is given by:

$$\rho_e(x) = -\frac{2e}{\pi}\partial_x\phi_b + 2e\frac{e^{i\pi\frac{x}{a}}}{\pi a} \cos 2\phi_b. \quad (12)$$

In the gapped regime,  $\langle\phi_b\rangle = 0$ , and the ground state of this system is formed of singlet pairs in a charge ordered state as represented in Figure 7. We therefore see that in the regime of strong interaction, both  $J_\perp$  and  $V_\perp$  will induce a charge ordering. However,  $J_\perp$  favors a phase with stripes formed along the rungs of the system, whereas  $V_\perp$  favors a zig-zag charge ordering. As a result, the competition between  $J_\perp$  and  $V_\perp$  induces a frustration in the system that can lead to a variety of charge ordering patterns.

### 3 Bosonization description

In the present section, we derive a bosonized representation of the Hamiltonian (1-2) in the limit  $J_\perp, V_\perp \ll t$ . For  $J_\perp = V_\perp = 0$ , the chains are decoupled, and the Hamiltonian describing their low energy, long wavelength excitations reads:

$$H = \sum_{p=1,2} H_{\rho,p} + H_{\sigma,p} \quad (13)$$

$$H_{\rho,p} = \int dx \left[ u_\rho K_\rho (\pi\Pi_{\rho,p})^2 + \frac{u_\rho}{K_\rho} (\partial_x\phi_{\rho,p})^2 \right] \quad (14)$$

$$H_{\sigma,p} = \int dx \left[ u_\sigma K_\sigma (\pi\Pi_{\sigma,p})^2 + \frac{u_\sigma}{K_\sigma} (\partial_x\phi_{\sigma,p})^2 \right] \quad (15)$$

where the fields satisfy to canonical commutation relations  $[\phi_{\nu,p}(x), \Pi_{\nu',p'}(x')] = i\delta_{\nu,\nu'}\delta_{p,p'}\delta(x-x')$ , ( $\nu = \rho, \sigma$ ). Since we do not assume  $U, V_\parallel \ll t$ , we use the renormalized values of  $u_\rho, K_\rho, u_\sigma, K_\sigma$  in the bosonized Hamiltonian of the decoupled chains (14-15). Spin rotational invariance imposes the renormalized value of  $K_\sigma = 1$ . The renormalized values of the remaining quantities can be obtained from the Bethe ansatz [65-68] for the Hubbard model or the t-J model at the supersymmetric point, or from numerical calculations in the case of a non-integrable model [69-71].

#### 3.1 Derivation of interchain coupling

In Section 2.1 we have seen that the  $4k_F$  harmonics in the fermion density play a crucial role for  $U/t \gg 1$ . The expression of the  $4k_F$  harmonics in terms of the boson fields can be obtained from references [72, 73]:

$$\rho_r(x) = -\frac{\sqrt{2}}{\pi}\partial_x\phi_{\rho_r} + \frac{e^{i(\sqrt{2}\phi_{\rho_r}-2k_Fx)}}{\pi a} \cos\sqrt{2}\phi_{\sigma_r}(x) + \frac{C}{\pi a} e^{i2(\sqrt{2}\phi_{\rho_r}-2k_Fx)}, \quad (16)$$

where  $r = 1, 2$  and  $k_F = \frac{\pi}{4a}$ . For  $U \rightarrow \infty$ , we recover the bosonized expression (9) of the density of spinless fermions with  $k'_F = 2k_F$ ,  $\phi = \sqrt{2}\phi_\rho$  and  $K = 2K_\rho$ . Using the expression (16) of the fermion density, we obtain the bosonized expression of the interchain repulsion  $V_\perp$ :

$$H_{V_\perp} = V_\perp a \int dx \left[ \frac{2}{\pi^2} \partial_x\phi_{\rho_1} \partial_x\phi_{\rho_2} + \frac{2}{(\pi a)^2} \cos\sqrt{2}(\phi_{\rho_1} - \phi_{\rho_2}) \cos\sqrt{2}\phi_{\sigma_1} \cos\sqrt{2}\phi_{\sigma_2} + \frac{C^2}{(\pi a)^2} \cos\sqrt{8}\phi_{\rho_1} \cos\sqrt{8}\phi_{\rho_2} \right]. \quad (17)$$

To obtain the bosonized expression of the spin exchange interaction, we need the spin density operators:

$$S_p^x(x) = \frac{1}{\pi a} \cos\sqrt{2}\theta_{\sigma,p}(x) \cos\sqrt{2}\phi_{\sigma,p}(x) + \frac{e^{i\sqrt{2}\phi_{\rho,p}-2k_Fx}}{2\pi a} \cos\sqrt{2}\theta_{\sigma,p}(x), \quad (18)$$

$$S_p^y(x) = \frac{1}{\pi a} \sin\sqrt{2}\theta_{\sigma,p}(x) \cos\sqrt{2}\phi_{\sigma,p}(x) + \frac{e^{i\sqrt{2}\phi_{\rho,p}-2k_Fx}}{2\pi a} \sin\sqrt{2}\theta_{\sigma,p}(x), \quad (19)$$

$$S_p^z(x) = -\frac{1}{\pi\sqrt{2}}\partial_x\phi_{\sigma,p} + \frac{e^{i\sqrt{2}\phi_{\rho,p}-2k_Fx}}{2\pi a} \sin\sqrt{2}\phi_{\sigma,p}(x), \quad (20)$$

where  $\theta_{\nu,p} = \pi \int^x \Pi_{\nu,p}(x') dx'$ . Since the terms coming from the  $4k_F$  harmonics are less relevant than those produced by the  $2k_F$  harmonics, in equations (18-20) we have altogether neglected the  $4k_F$  harmonics, whose expression can be found in the Appendix B. From the bosonized expression of the spin densities, we obtain the exchange interaction as:

$$H_{J_\perp} = \frac{J_\perp}{2\pi^2} \int dx \partial_x\phi_{\sigma,1} \partial_x\phi_{\sigma,2} + \frac{J_\perp}{2(\pi a)^2} \int dx \cos\sqrt{2}(\theta_{\sigma,1} - \theta_{\sigma,2}) \cos\sqrt{2}(\phi_{\sigma,1} + \phi_{\sigma,2}) + \frac{J_\perp}{(2\pi a)^2} \int dx \cos\sqrt{2}(\phi_{\rho,1} - \phi_{\rho,2}) \left[ 2 \cos\sqrt{2}(\theta_{\sigma,1} - \theta_{\sigma,2}) + \cos\sqrt{2}(\phi_{\sigma,1} - \phi_{\sigma,2}) - \sqrt{2}(\phi_{\sigma,1} + \phi_{\sigma,2}) \right]. \quad (21)$$

The total interchain interaction Hamiltonian  $H_\perp = H_{V_\perp} + H_{J_\perp}$ , is more conveniently written by introducing

the new canonically conjugate fields [74]  $\phi_{\nu,\pm} = (\phi_{\nu,1} \pm \phi_{\nu,2})/\sqrt{2}$  and  $\Pi_{\nu,\pm} = (\Pi_{\nu,1} \pm \Pi_{\nu,2})/\sqrt{2}$ , as:

$$\begin{aligned}
 H_{\perp} = & \frac{(4V_{\perp} + J_{\perp})a}{(2\pi a)^2} \int dx \cos 2\phi_{\rho-} \cos 2\phi_{\sigma-} \\
 & + \frac{(4V_{\perp} - J_{\perp})a}{(2\pi a)^2} \int dx \cos 2\phi_{\rho-} \cos 2\phi_{\sigma+} \\
 & + \frac{2J_{\perp}a}{(2\pi a)^2} \int dx \cos 2\phi_{\rho-} \cos 2\theta_{\sigma-} \\
 & + \frac{2C^2V_{\perp}a}{(2\pi a)^2} \int dx (\cos 4\phi_{\rho-} + \cos 4\phi_{\rho+}) \\
 & + \frac{V_{\perp}}{\pi^2} \int dx [(\partial_x \phi_{\rho+})^2 - (\partial_x \phi_{\rho-})^2] \\
 & + \frac{J_{\perp}}{4\pi^2} \int dx [(\partial_x \phi_{\sigma+})^2 - (\partial_x \phi_{\sigma-})^2]. \quad (22)
 \end{aligned}$$

From the bosonized expression (22) of the interchain interactions and the Hamiltonians of the decoupled chains (14–15) we obtain the full bosonized form of the Hamiltonian (1–2). The total charge mode  $\phi_{\rho+}$  decouples from the spin and staggered charge modes. Below, we will start discussing the properties of the Hamiltonians of these modes.

### 3.2 Total charge Hamiltonian

The total charge excitation Hamiltonian is:

$$\begin{aligned}
 H_{\rho+} = & \int \frac{dx}{2\pi} \left[ u_{\rho+} K_{\rho+} (\pi \Pi_{\rho+})^2 + \frac{u_{\rho+}}{K_{\rho+}} (\partial_x \phi_{\rho+})^2 \right] \\
 & + \frac{2g_0}{(2\pi a)^2} \int dx \cos 4\phi_{\rho+}, \quad (23)
 \end{aligned}$$

where:

$$u_{\rho+} = u_{\rho} \left( 1 + \frac{2K_{\rho}V_{\perp}a}{\pi u_{\rho}} \right)^{\frac{1}{2}} \quad (24)$$

$$K_{\rho+} = K_{\rho} \left( 1 + \frac{2K_{\rho}V_{\perp}a}{\pi u_{\rho}} \right)^{-\frac{1}{2}} \quad (25)$$

$$g_0 = C^2 V_{\perp}. \quad (26)$$

The expression of the interchain coupling  $g_0$  in (23) can also be derived in perturbation theory by the approach of reference [14] and a sketch of such derivation can be found in the Appendix A. We note that the same sine-Gordon Hamiltonian was derived in Section 2.1 in the limit  $U/t \rightarrow \infty$ , with the identification  $\phi_{+} = \sqrt{2}\phi_{\rho}$ ,  $K = 2K_{\rho}$ ,  $K_{+} = 2K_{\rho+}$ , and  $C = 1$ . A similar Hamiltonian was also obtained in Section 2.2 in the limit  $J_{\perp} \rightarrow \infty$ . This fact indicates a continuity relation between the weak and the

strong coupling regimes for the charge excitations. Finally, the Hamiltonian for the total charge mode (23) can also be recovered from a general argument [19, 75]: From equation (16), it is easily seen that a translation by one lattice site amounts to making  $\sqrt{2}\phi_{\rho,n} \rightarrow \sqrt{2}\phi_{\rho,n} - \pi/2$ , and thus  $\phi_{\rho+} \rightarrow \phi_{\rho+} - \pi/2$ . Translation invariance of the lattice Hamiltonian requires the continuum bosonized Hamiltonian to be invariant under such transformation. The most relevant Umklapp operator compatible with this symmetry is  $\cos 4\phi_{\rho+}$ , and it should be the operator responsible for the opening of the gap in the charge modes at quarter-filling. As a result, in the strong coupling regime, we find a boundary between the gapped and the gapless regime given by  $K_{\rho+} = 1/2$ . Concerning the intrachain Umklapp terms, they are of the form [12, 13]  $\cos 4\sqrt{2}\phi_{1,2}$  and become relevant only for  $K_{\rho} < 1/4$ . Thus we can safely neglect them compared with interchain Umklapp terms. A final remark is in order concerning the sign of  $g_0$ . In Appendix B, we show that the interaction in the spin sector only produces a term of the form  $\cos 4\phi_{\rho+} \cos 2\theta_{\sigma-} \cos 2\phi_{\sigma+}$ . This latter term is less relevant than a term of the form  $\cos 4\phi_{\rho+}$ , so that we can usually neglect it and assume  $g_0 > 0$ . However, if the spin gap in the system is large, this term cannot be neglected and contributes a correction  $\cos 4\phi_{\rho+} \langle \cos 2\theta_{\sigma-} \cos 2\phi_{\sigma+} \rangle$  to the Hamiltonian (23). This can result in a change of the sign of  $g_0$ . In that case, instead of having  $\langle \phi_{\rho+} \rangle = \frac{\pi}{4}$  in the ground state, we should have instead  $\langle \phi_{\rho+} \rangle = 0$ . In the following we will discuss both the phases with  $\langle \phi_{\rho+} \rangle = \frac{\pi}{4}$  and  $\langle \phi_{\rho+} \rangle = 0$ . The latter ones are expected to be obtained when  $J_{\perp} \gg V_{\perp}$  since we need a large spin gap to modify the sign of  $g_0$ .

### 3.3 Spin and charge difference Hamiltonian

From equations (14–15) and equation (22), we obtain the Hamiltonian describing the interaction of spin modes  $\phi_{\sigma\pm}$  and interchain charge modes  $\phi_{\rho-}$ . Under renormalization group (RG) transformation, besides the interactions already present in the bare Hamiltonians, new interactions can be generated. Thus the Hamiltonian to consider reads:

$$\begin{aligned}
 \tilde{H} = & H_{\rho-} + H_{\sigma+} + H_{\sigma-} \\
 = & \int \frac{dx}{2\pi} \sum_{\nu \in \{\rho-, \sigma+, \sigma-\}} \left[ u_{\nu} K_{\nu} (\pi \Pi_{\nu})^2 + \frac{u_{\nu}}{K_{\nu}} (\partial_x \phi_{\nu})^2 \right] \\
 & + \frac{2g_1}{(2\pi a)^2} \int dx \cos 2\phi_{\sigma+} \cos 2\phi_{\sigma-} \\
 & + \frac{2g_2}{(2\pi a)^2} \int dx \cos 2\phi_{\sigma+} \cos 2\theta_{\sigma-} \\
 & + \frac{2g_3}{(2\pi a)^2} \int dx \cos 4\phi_{\rho-} \\
 & + \frac{2g_4}{(2\pi a)^2} \int dx \cos 2\phi_{\rho-} \cos 2\phi_{\sigma+} \\
 & + \frac{2g_5}{(2\pi a)^2} \int dx \cos 2\phi_{\rho-} \cos 2\phi_{\sigma-} \\
 & + \frac{2g_6}{(2\pi a)^2} \int dx \cos 2\phi_{\rho-} \cos 2\theta_{\sigma-}, \quad (27)
 \end{aligned}$$

where:

$$u_{\rho-} = u_{\rho} \left( 1 - \frac{2V_{\perp} K_{\rho} a}{\pi u_{\rho}} \right)^{1/2} \quad (28)$$

$$u_{\sigma+} = u_{\sigma} \left( 1 + \frac{J_{\perp} a}{2\pi u_{\rho}} \right)^{1/2}, \quad u_{\sigma-} = u_{\sigma} \left( 1 - \frac{J_{\perp} a}{2\pi v_F} \right)^{1/2}, \quad (29)$$

$$K_{\rho-} = K_{\rho} \left( 1 - \frac{2V_{\perp} K_{\rho} a}{\pi u_{\rho}} \right)^{-1/2}, \quad (30)$$

$$K_{\sigma+} = \left( 1 + \frac{J_{\perp} a}{2\pi v_F} \right)^{-1/2}, \quad K_{\sigma-} = \left( 1 - \frac{J_{\perp} a}{2\pi v_F} \right)^{-1/2}, \quad (31)$$

$$g_1 = 0, \quad g_2 = J_{\perp} a, \quad g_3 = 2C^2 V_{\perp} a, \quad (32)$$

$$g_4 = (2V_{\perp} - \frac{J_{\perp}}{2})a, \quad g_5 = (2V_{\perp} + \frac{J_{\perp}}{2})a, \quad g_6 = J_{\perp} a. \quad (33)$$

Note that in equations (28), we have put  $g_1 = 0$  because the intrachain spin interaction in the repulsive Hubbard model are marginally irrelevant. In full rigor, we should have added a small marginally irrelevant interaction to the Hamiltonian (15) and we would have obtained  $g_1 > 0$  and slightly modified expressions of  $K_{\sigma\pm}$ . In spite of the fact that we have put  $g_1 = 0$  in the initial conditions, in the following we will also discuss the case of a relevant  $g_1$  under RG. We also note that the Hamiltonian (27) possesses a discrete global gauge invariance under the simultaneous transformation:

$$\begin{aligned} \phi_{\sigma\pm} &\rightarrow \phi_{\sigma\pm} + \frac{\pi}{2} \\ \theta_{\sigma-} &\rightarrow \theta_{\sigma-} + \frac{\pi}{2} \\ \phi_{\rho-} &\rightarrow \phi_{\rho-} + \frac{\pi}{2}. \end{aligned} \quad (34)$$

To study the Hamiltonian (27) RG equations can be derived. Velocity differences between the various modes can be neglected, and one can take  $u_{\sigma\pm} = u_{\rho-} = v_F$ . Introducing  $y_i = g_i/(\pi v_F)$  and  $K_{\sigma r} = 1 + y_{\sigma r}/2$ , and using the operator product expansion (OPE) methods [76], the RG equations read:

$$\frac{d}{dl} \left( \frac{1}{K_{\rho-}} \right) = y_3^2 + \frac{1}{8}(y_4^2 + y_5^2 + y_6^2), \quad (35)$$

$$\frac{dy_{\sigma-}}{dl} = \frac{1}{4}(y_6^2 + y_2^2 - y_1^2 - y_5^2), \quad (36)$$

$$\frac{dy_{\sigma+}}{dl} = -\frac{1}{4}(y_1^2 + y_2^2 + y_4^2), \quad (37)$$

$$\frac{dy_1}{dl} = -\frac{1}{2}[(y_{\sigma+} + y_{\sigma-})y_1 + y_4 y_5], \quad (38)$$

$$\frac{dy_2}{dl} = -\frac{1}{2}[(y_{\sigma+} - y_{\sigma-})y_2 + y_4 y_6], \quad (39)$$

$$\frac{dy_3}{dl} = (2 - 4K_{\rho-})y_3 - \frac{1}{8}(y_4^2 + y_5^2 + y_6^2), \quad (40)$$

$$\frac{dy_4}{dl} = (1 - K_{\rho-})y_4 - \frac{1}{2}(y_{\sigma+} y_4 + y_1 y_5 + y_2 y_6 + y_3 y_4), \quad (41)$$

$$\frac{dy_5}{dl} = (1 - K_{\rho-})y_5 - \frac{1}{2}(y_{\sigma-} y_5 + y_3 y_5 + y_1 y_4), \quad (42)$$

$$\frac{dy_6}{dl} = (1 - K_{\rho-})y_6 + \frac{1}{2}(y_{\sigma-} y_6 - y_3 y_6 - y_2 y_4). \quad (43)$$

We see from these equations that although  $y_1$  is initially zero, it becomes non-zero under the RG flow. The fact that the problem under consideration has  $SU(2)$  spin rotational invariance leads to a simplification of the RG equations (35–43). The initial conditions (28–33) lead to the following relations  $\forall l$ :

$$y_{\sigma+}(l) + y_{\sigma-}(l) = y_1(l), \quad (44)$$

$$y_{\sigma-}(l) - y_{\sigma+}(l) = y_2(l), \quad (45)$$

$$y_5(l) - y_4(l) = y_6(l). \quad (46)$$

These conditions ensure the  $SU(2)$  symmetry of the RG flow and reduce the flow from a curve in a nine-dimensional space to a curve in a six-dimensional hyperplane. The simplified RG equations now reads:

$$\frac{d}{dl} \left( \frac{1}{K_{\rho-}} \right) = y_3^2 + \frac{1}{4}(y_4^2 + y_6^2 + y_4 y_6)$$

$$\frac{dy_1}{dl} = -\frac{1}{2}(y_1^2 + y_4^2 + y_4 y_6)$$

$$\frac{dy_2}{dl} = \frac{1}{2}(y_2^2 - y_4 y_6)$$

$$\frac{dy_3}{dl} = (2 - 4K_{\rho-})y_3 - \frac{1}{4}(y_4^2 + y_6^2 + y_4 y_6)$$

$$\begin{aligned} \frac{dy_4}{dl} &= (1 - K_{\rho-})y_4 - \frac{1}{4}(3y_1 y_4 - y_2 y_4 \\ &\quad + 2y_2 y_6 + 2y_1 y_6 + 2y_3 y_4) \end{aligned}$$

$$\frac{dy_6}{dl} = (1 - K_{\rho-})y_6 + \frac{1}{4}(y_1 y_6 + y_2 y_6 - 2y_3 y_6 - 2y_2 y_4). \quad (47)$$

The flow of these equations will be discussed in Section 6. Here, we want to discuss briefly the possible fixed points within a semiclassical argument, *i.e.* by considering the expectation values of the phase fields that minimize the classical ground state energy. By looking at the possible classical minima, we can distinguish two regimes. In the first regime,  $\langle \phi_{\rho-} \rangle = 0, \frac{\pi}{2}$  and  $\langle \cos 2\phi_{\rho-} \rangle \neq 0$ . This case is similar to that obtained in ladders at incommensurate filling [30, 31, 74]. In this regime the relevance of the terms  $g_{4,5,6}$  is responsible for the presence of the spin gap. In the second regime,  $\langle \phi_{\rho-} \rangle = \pm \frac{\pi}{4}$ , so that  $\langle \cos 4\phi_{\rho-} \rangle \neq 0$ , and  $\langle \cos 2\phi_{\rho-} \rangle = 0$ . This regime corresponds to  $g_3$  being the dominant interaction, and  $g_{4,5,6}$  being less relevant interactions. This case is specific of the quarter-filled ladder, and corresponds in the limit  $U = \infty$  of Section 2.1 to the formation of the gap in  $\phi_{-}$ . We note that in the present regime, spin gaps can also be generated by the  $g_{1,2}$  terms. When  $g_1$  is the relevant interaction, the corresponding bosonized expression can be rewritten as  $\sim g_1(\cos \sqrt{8}\phi_1 + \cos \sqrt{8}\phi_2)$ , so that the spin gaps correspond to two independent intrachain spin gaps. We also note that in order to preserve spin rotational invariance, we need to have  $g_1 < 0$  in that case.

It is possible to give a roughly estimate of the parameters region where each regime dominate by looking at the scaling dimensions of the operators. The operator  $\cos 4\phi_{\rho-}$  has scaling dimension  $4K_{\rho-}$  so that it is relevant for  $K_{\rho-} < 1/2$ . The operators  $\cos 2\phi_{\rho-} \cos 2\phi_{\sigma-}$ ,  $\cos 2\phi_{\rho-} \cos 2\phi_{\sigma+}$ ,  $\cos 2\phi_{\rho-} \cos 2\theta_{\sigma-}$  have respective scaling dimensions  $K_{\rho-} + K_{\sigma-}$ ,  $K_{\rho-} + K_{\sigma+}$ ,  $K_{\rho-} + 1/K_{\sigma-}$ . Taking into account the spin rotational symmetry, this implies that these operators have all the dimension  $K_{\rho-} + 1$  and become relevant for  $K_{\rho-} < 1$ . The operator  $\cos 4\phi_{\rho-}$  becomes the most relevant operator when  $4K_{\rho-} < 1 + K_{\rho-}$ , *i.e.* for  $K_{\rho-} < 1/3$ . Therefore, we expect to have the first regime in the limit of a repulsion not too strong,  $1/3 < K_{\rho-} < 1/2$ , and the second regime in the case of a stronger repulsion  $1/4 < K_{\rho-} < 1/2$ .

## 4 Phase diagram

In this section, we describe the various insulating phases predicted from the renormalization group equations (47). In order to describe the possible ground states in the phase diagram, we introduce first the corresponding order parameters.

### 4.1 Order parameters

Since for strong repulsion the system has a gap in the spin excitations, the possible order parameters can only be bond-order waves (BOW) and charge density waves (CDW). We will denote the corresponding phases as  $(q_x, q_y)$ -BOW, and  $(q_x, q_y)$ -CDW where  $q_x = \pi/2$  or  $\pi$  and  $q_y = 0, \pi$  or  $q_y = \pm\pi/2$  if  $q_x = \pi/2$ . The phases with a  $q_x = \pi$  ordering have at least two-fold degenerate ground state, while the phases with a  $q_x = \pi/2$  have a four-fold degenerate ground state.

On the lattice, these operators are defined as:

$$O_{\text{CDW}(\pi, q_y)}(i) = (-)^i (n_{i,1} + \cos(q_y) n_{i,2}) (q_y = 0, \pi) \quad (48)$$

$$O_{\text{BOW}(\pi, q_y)}(i) = (-)^i \sum_{\sigma} (c_{i+1,1,\sigma}^{\dagger} c_{i+1,1,\sigma}^{\dagger} + \cos(q_y) c_{i+1,2,\sigma}^{\dagger} c_{i+1,2,\sigma}^{\dagger}) (q_y = 0, \pi) \quad (49)$$

$$O_{\text{CDW}(\frac{\pi}{2}, q_y)}(i) = e^{-i\frac{\pi}{2}i} (e^{iq_y/2} n_{i,1} + e^{-iq_y/2} n_{i,2}) (q_y = 0, \frac{\pi}{2}, \pi, -\frac{\pi}{2}). \quad (50)$$

The corresponding bosonized expressions is obtained by those of the charge densities as a function of  $\phi_{\rho\pm}$  and  $\phi_{\sigma 1,2}$ :

$$\rho_1(x) = -\frac{1}{\pi} \partial_x (\phi_{\rho+} + \phi_{\rho-}) + \frac{e^{i(\phi_{\rho+} + \phi_{\rho-} - 2k_F x)}}{\pi a} \times \cos \sqrt{2} \phi_{\sigma_1}(x) + \frac{C}{\pi a} e^{2i(\phi_{\rho+} + \phi_{\rho-} - 2k_F x)}, \quad (51)$$

$$\rho_2(x) = -\frac{1}{\pi} \partial_x (\phi_{\rho+} - \phi_{\rho-}) + \frac{e^{i(\phi_{\rho+} - \phi_{\rho-} - 2k_F x)}}{\pi a} \times \cos \sqrt{2} \phi_{\sigma_2}(x) + \frac{C}{\pi a} e^{2i(\phi_{\rho+} - \phi_{\rho-} - 2k_F x)}. \quad (52)$$

We consider first  $q_x = \pi$ . The charge density wave order parameters are straightforwardly obtained from (51–52) as:

$$O_{\text{CDW}(\pi, 0)} \sim \frac{1}{2\pi\alpha} \cos 2\phi_{\rho+} \cos 2\phi_{\rho-} \quad (53)$$

$$O_{\text{CDW}(\pi, \pi)} \sim \frac{1}{2\pi\alpha} \sin 2\phi_{\rho+} \sin 2\phi_{\rho-}. \quad (54)$$

The bond order wave order parameters measure the charge density between the sites  $i$  and  $i + 1$ , *i.e.* on site  $i + 1/2$ , and their bosonized expression reads:

$$O_{\text{BOW}(\pi, 0)} \sim \frac{1}{2\pi\alpha} \sin 2\phi_{\rho+} \cos 2\phi_{\rho-} \quad (55)$$

$$O_{\text{BOW}(\pi, \pi)} \sim \frac{1}{2\pi\alpha} \cos 2\phi_{\rho+} \sin 2\phi_{\rho-}. \quad (56)$$

Concerning the  $\pi/2$  charge density wave order parameter, we have to consider whether  $\phi_{\sigma-}$  or  $\theta_{\sigma-}$  is ordered. In the case  $\theta_{\sigma-}$  is ordered, the operators  $\cos \sqrt{2} \phi_{\sigma,1,2}$  have zero expectation value, and exponentially decaying correlations, so that all of the  $(\pi/2, q_y)$ -CDW order parameters have short-range order. When  $\phi_{\sigma-}$  and  $\phi_{\sigma+}$  are ordered, the operators  $\cos \sqrt{2} \phi_{\sigma,1,2}$  have non-zero expectation values. In this case, the expression of the order parameters for  $(\pi/2, q_y)$ -CDW as a function of  $\phi_{\rho+}$  and  $\phi_{\rho-}$  is:

$$O_{\text{CDW}(\frac{\pi}{2}, 0)} \sim \frac{1}{2\pi\alpha} e^{i\phi_{\rho+}} \cos \phi_{\rho-} \quad (57)$$

$$O_{\text{CDW}(\frac{\pi}{2}, \frac{\pi}{2})} \sim \frac{1}{2\pi\alpha} e^{i\phi_{\rho+}} \cos \left( \phi_{\rho-} - \frac{\pi}{4} \right) \quad (58)$$

$$O_{\text{CDW}(\frac{\pi}{2}, \pi)} \sim \frac{1}{2\pi\alpha} e^{i\phi_{\rho+}} \sin \phi_{\rho-} \quad (59)$$

$$O_{\text{CDW}(\frac{\pi}{2}, -\frac{\pi}{2})} \sim \frac{1}{2\pi\alpha} e^{i\phi_{\rho+}} \cos \left( \phi_{\rho-} + \frac{\pi}{4} \right). \quad (60)$$

From the knowledge of the order parameters, in the following we are going to discuss the ground states that are realized for the various possible ordering of the phase fields. We will first discuss the orderings with  $\langle \phi_{\rho-} \rangle = \frac{\pi}{4}$  and then turn to orderings with  $\langle \phi_{\rho-} \rangle = 0$ . As we have explained in Section 3.2, the latter type of ordering should be expected for dominant  $J_{\perp}$ . In Tables 1–2 we give a summary of the phases corresponding to  $\langle \phi_{\rho+} \rangle = 0$  and  $\langle \phi_{\rho+} \rangle = \frac{\pi}{4}$ . These different phases are detailed in the forthcoming sections.

### 4.2 $(\pi, \pi)$ -charge density wave

In the case of  $\langle \phi_{\rho+} \rangle = \frac{\pi}{4}$ ,  $\langle \phi_{\rho-} \rangle = \frac{\pi}{4}$ ,  $\langle \phi_{\sigma+} \rangle = 0$ ,  $\langle \theta_{\sigma-} \rangle = \frac{\pi}{2}$  (up to a discrete gauge transformation (34)), the  $(\pi/2, q_y)$ -CDW order parameters have all zero expectation value and exponentially decaying correlations. Moreover, the  $(\pi, \pi)$ -CDW order parameter has a non-zero expectation value, leading to a zig-zag charge ordering [41, 48]. This ordering is represented in Figure 1. This charge ordered phase possesses also a spin gap caused by interchain coupling and identifies with the CDW<sub>sg</sub> (with

**Table 1.** The phases of the quarter-filled ladder in the case  $\langle\phi_{\rho+}\rangle = 0$ . The locking positions are given up to a global gauge transformation (34).

$\langle\phi_{\rho+}\rangle = \mathbf{0}$	$\langle\phi_{\rho-}\rangle$	$\langle\phi_{\sigma+}\rangle$	$\langle\phi_{\sigma-}\rangle$	$\langle\theta_{\sigma-}\rangle$
$(\frac{\pi}{2}, \pi)$ -CDW	$\pm\frac{\pi}{2}$	0	0	-
$(\pi, 0)$ -CDW	$\pm\frac{\pi}{2}$	$\pm\frac{\pi}{2}$	-	0
$(\pi, \pi)$ -BOW	$\pm\frac{\pi}{4}$	0	-	$\pm\frac{\pi}{2}$
$(\frac{\pi}{2}, \frac{\pi}{2})$ -CDW	$\pm\frac{\pi}{4}$	0	0	-
$(\pi, \pi)$ -BOW	$\pm\frac{\pi}{4}$	0	0	-

**Table 2.** The phases of the quarter-filled ladder in the case  $\langle\phi_{\rho+}\rangle = \frac{\pi}{4}$ . The locking positions are given up to a global gauge transformation (34).

$\langle\phi_{\rho+}\rangle = \frac{\pi}{4}$	$\langle\phi_{\rho-}\rangle$	$\langle\phi_{\sigma+}\rangle$	$\langle\phi_{\sigma-}\rangle$	$\langle\theta_{\sigma-}\rangle$
$(\frac{\pi}{2}, \pi)$ -CDW	$\pm\frac{\pi}{2}$	0	0	-
$(\pi, 0)$ -BOW	$\pm\frac{\pi}{2}$	$\pm\frac{\pi}{2}$	-	0
$(\pi, \pi)$ -CDW	$\pm\frac{\pi}{4}$	0	-	$\pm\frac{\pi}{2}$
$(\frac{\pi}{2}, \frac{\pi}{2})$ -CDW	$\pm\frac{\pi}{4}$	0	0	-
$(\pi, \pi)$ -CDW	$\pm\frac{\pi}{4}$	0	0	-

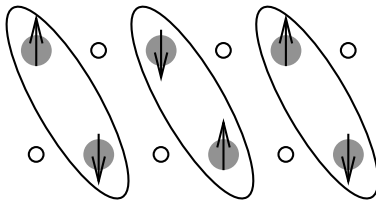


**Fig. 1.** The phase with zig-zag charge ordering and spin gap  $(\pi, \pi)$ -CDW. The grey circles represent the local charge density and the arrows the spins. The empty circles indicate the absence of spin or charge on that site. The ovals represent the formation of interchain spin singlets.

spin gap) of reference [48]. The ground state is this phase is fourfold degenerate (twofold due to translation symmetry, and twofold due to the two possible orientations of the spin singlets). We note that this phase has previously been discussed in Section 2.1 in the limit of  $U \rightarrow \infty$ , however in that limit it was not possible to discuss the spin modes. From the discussion of Section 2.1, we see that the essential ingredient for the zig-zag ordering is the mutual locking of the  $4k_F$  charge density fluctuations so that zig-zag ordering needs both strong intrachain and interchain repulsion. The formation of the spin gap appears to be unrelated to the zig-zag ordering, but only a consequence of the coupling of the  $q = 0$  fluctuations. We note however that the higher order terms derived in Appendix B could lead in the case of a large charge gap to corrections to the spin Hamiltonian that could enhance the spin gap. In

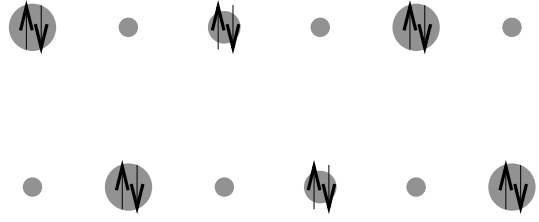


**Fig. 2.** The  $(\frac{\pi}{2}, \frac{\pi}{2})$ -charge density wave phase. The grey circles represent the local charge density. The difference in diameter indicates small or large charge density on that site. Pairs of arrows pointing in opposite directions indicate the formation of intrachain spin singlets.

the RG study of equations (35), this phase is obtained for  $y_3 \rightarrow +\infty$ , and  $y_2 \rightarrow +\infty$ .

### 4.3 $(\frac{\pi}{2}, \frac{\pi}{2})$ charge density wave

In the case of  $\langle\phi_{\rho+}\rangle = \langle\phi_{\rho-}\rangle = \pm\frac{\pi}{4}$  and  $\langle\phi_{\sigma+}\rangle = 0$ ,  $\langle\phi_{\sigma-}\rangle = 0$  a  $(\frac{\pi}{2}, \pm\frac{\pi}{2})$ -CDW state is formed coexisting with a  $(\pi, \pi)$ -CDW oscillation. This phase possesses also an intrachain spin gap. The corresponding state is represented in Figure 2. A simple physical picture of this state is that a  $\frac{\pi}{2}$ -charge density is formed in each chain, and the interchain repulsion locks the phases of both charge density waves. Since there is an intrachain gap, this phase appears to be more likely to be observed in a Hubbard ladder with  $U < 0$  and  $V_{\parallel} > 0$  or in a t-J ladder in a regime in which  $J_{\parallel}$  is large enough to cause the formation of a spin gap in the single chain [71]. The dephasing between the two charge density waves is  $2\langle\phi_{\rho-}\rangle = \pm\frac{\pi}{2}$ . This dephasing results from the mutual locking of the  $4k_F$  density fluctuations, thus pointing to strong repulsion in the chain. The corresponding phase has a fourfold degenerate ground state. In the renormalization group treatment, this phase is obtained for  $y_1 \rightarrow -\infty$  and  $y_3 \rightarrow +\infty$ .

### 4.4 $(\pi, 0)$ bond order wave

For  $\langle\phi_{\rho+}\rangle = \frac{\pi}{4}$ ,  $\langle\phi_{\rho-}\rangle = \frac{\pi}{2}$ ,  $\langle\phi_{\sigma+}\rangle = \frac{\pi}{2}$ ,  $\langle\theta_{\sigma-}\rangle = 0$ , all of the CDW order parameters vanish. The only nonvanishing order parameter is  $(\pi, 0)$ -BOW. This BOW can be described in physical terms in the following way: the fermions are localized on the bonds between two sites, and due to the  $J_{\perp}$  interaction, they form a spin singlet with the fermion on the opposite chain. Clearly, this phase should be expected at strong  $J_{\perp}$  and moderate repulsion in the chains. The ground state is only twofold degenerate. In the renormalization group, this phase is obtained for  $y_4 \rightarrow -\infty$ ,  $y_5 + y_6 \rightarrow +\infty$ , and the inspection of the expression of  $y_4$  confirms that  $J_{\perp}$  is the dominant interaction in the  $(\pi, 0)$ -BOW. The corresponding phase is drawn in Figure 3. We note that since this phase has a uniform charge density, it is a possible candidate for the homogeneous insulator  $\text{HI}_{\text{sg}}$  phase of reference [48]. It is also interesting to remark that this phase is a two-leg analog

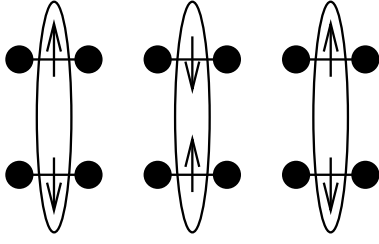


**Fig. 3.** The  $(\pi, 0)$ -bond-order wave phase. The connected black circles represent a bond occupied by an electron. Arrows indicate the spin of the electrons. Ovals represent the formation of interchain singlet state as in Figure 1.

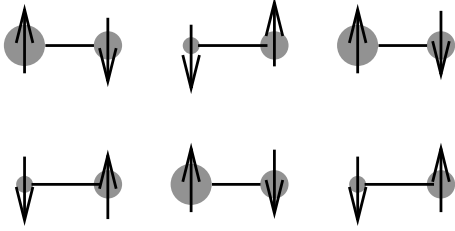


**Fig. 4.** The  $(\frac{\pi}{2}, \pi)$ -CDW with  $(\pi, 0)$ -BOW. The grey circles represent the charge density in Figure 2 and the black horizontal lines denote occupied bonds as in Figure 3. Arrows represent electron spins, and the black horizontal line indicate that the spins are bound in an intrachain singlet. In contrast with the pure  $(\pi, 0)$ -BOW the charge density is inhomogeneous along the chains.

of the  $SDW_1$  phase obtained in [77] in a system of coupled quarter filled extended Hubbard chains.

#### 4.5 $(\frac{\pi}{2}, \pi)$ charge density wave

For  $\langle \phi_{\rho+} \rangle = \frac{\pi}{4}$ ,  $\langle \phi_{\rho-} \rangle = \frac{\pi}{2}$ ,  $\langle \phi_{\sigma+} \rangle = 0$ ,  $\langle \phi_{\sigma-} \rangle = 0$ , the  $(\frac{\pi}{2}, \pi)$ -CDW order parameter does not vanish. The  $(\pi, 0)$ -BOW correlations are also present in this phase. A sketch of this phase is given in Figure 4. Similarly to the  $(\frac{\pi}{2}, \frac{\pi}{2})$ -CDW this phase results from the mutual locking of the  $2k_F$  charge density wave fluctuations of the two coupled chains. However, in contrast to the  $(\frac{\pi}{2}, \frac{\pi}{2})$ -CDW this locking is produced by the coupling of the  $2k_F$  density fluctuations. This implies that the spin gap is formed as a result of interchain coupling. In the RG study this phase is obtained for  $y_4 \rightarrow +\infty$ ,  $y_5 + y_6 \rightarrow +\infty$ . Using the expression of  $y_4$  we see that this phase is dominated by interchain repulsion in contrast with the  $(\pi, 0)$ -BOW.

#### 4.6 $(\pi, \pi)$ bond order wave

When  $\langle \phi_{\rho+} \rangle = 0$ ,  $\langle \phi_{\rho-} \rangle = \pm \frac{\pi}{4}$ ,  $\langle \phi_{\sigma+} \rangle = 0$ ,  $\langle \theta_{\sigma-} \rangle = \frac{\pi}{2}$ , all of the CDW order parameters vanish and only the  $(\pi, \pi)$ -BOW order parameter is non-zero. This phase corresponds to a staggered bond ordering shown in Figure 5. It can be viewed as a  $(\pi, \pi)$ -CDW translated by half a lattice spacing. Elementary excitations in this phase are thus similar to those of the  $(\pi, \pi)$ -CDW phase. In the renormalization group such state is obtained for  $y_2 \rightarrow +\infty$ ,  $y_3 \rightarrow +\infty$ .

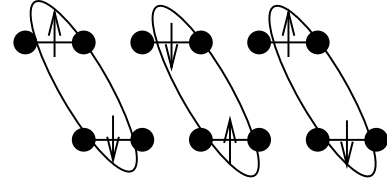


**Fig. 5.** Sketch of the  $(\pi, \pi)$ -BOW. The symbols have the same meaning as in Figure 3.

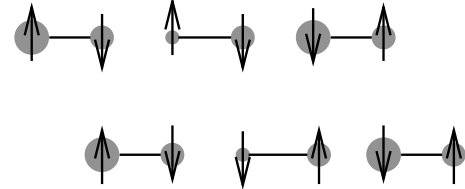


**Fig. 6.** The  $(\frac{\pi}{2}, \frac{\pi}{2})$ -CDW with  $(\pi, \pi)$ -BOW. The symbols have the same meaning as in Figure 4.

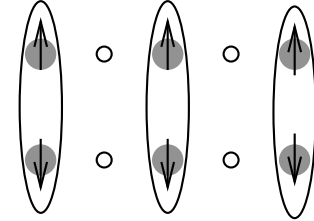


**Fig. 7.** The  $(\pi, 0)$ -CDW. The symbols have the same meaning as in Figure 1.

#### 4.7 $(\frac{\pi}{2}, \frac{\pi}{2})$ charge density wave

When  $\langle \phi_{\rho+} \rangle = 0$ ,  $\langle \phi_{\rho-} \rangle = \pm \frac{\pi}{4}$ ,  $\langle \phi_{\sigma+} \rangle = 0$ ,  $\langle \phi_{\sigma-} \rangle = 0$ , the  $(\frac{\pi}{2}, \frac{\pi}{2})$ -CDW order parameter does not vanish and coexists with a  $(\pi, \pi)$ -BOW. This phase is different from the  $(\frac{\pi}{2}, \frac{\pi}{2})$ -CDW previously encountered as the previous phase contained a  $(\pi, \pi)$ -CDW. There are however similarities between these two phases since both result from the mutual locking of  $4k_F$  components of density fluctuations combined with an intrachain spin gap. Since the sign change in  $g_0$  results from the formation of an interchain spin gap, we should expect this phase to have only a rather narrow domain of existence. This phase is sketched in Figure 6. In the renormalization group treatment, it is obtained when  $y_1 \rightarrow -\infty$ ,  $y_3 \rightarrow +\infty$ .

#### 4.8 $(\pi, 0)$ charge density wave

When  $\langle \phi_{\rho+} \rangle = 0$ ,  $\langle \phi_{\rho-} \rangle = \pm \frac{\pi}{2}$ ,  $\langle \phi_{\sigma+} \rangle = \frac{\pi}{2}$ ,  $\langle \theta_{\sigma-} \rangle = 0$ , the only non-vanishing order parameter is the  $(\pi, 0)$ -CDW one. In the RG study this phase is obtained for  $y_4 \rightarrow -\infty$ ,  $y_5 + y_6 \rightarrow +\infty$ , *i.e.* it corresponds to a dominant  $J_{\perp}$ , in agreement with the results of Section 2.2. This phase can be viewed as the  $(\pi, 0)$ -BOW shifted by a half lattice spacing. The corresponding phase is sketched in Figure 7.

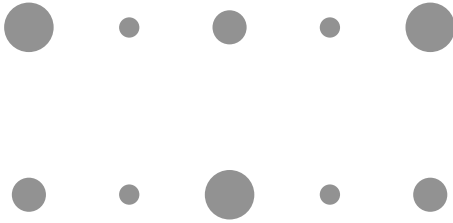


**Fig. 8.** The  $(\frac{\pi}{2}, \pi)$ -CDW with  $(\pi, 0)$ -CDW. The grey circles have the same meaning as in Figure 2. The formation of intrachain spin singlets has not been represented.

#### 4.9 $(\frac{\pi}{2}, \pi)$ charge density wave

When  $\langle \phi_{\rho+} \rangle = 0, \langle \phi_{\rho-} \rangle = \pm \frac{\pi}{2}, \langle \phi_{\sigma+} \rangle = 0, \langle \phi_{\sigma-} \rangle = 0$ , the only non-vanishing order parameters are the  $(\pi, 0)$ -CDW and the  $(\frac{\pi}{2}, \pi)$ -CDW ones. Under RG study, this phase is obtained for  $y_4 \rightarrow +\infty, y_5 + y_6 \rightarrow +\infty$  and corresponds to dominant  $V_{\perp}$ . For this reason, we should expect this phase to have a rather narrow domain of existence. The spin gap corresponds again to an intrachain spin gap. This phase is sketched in Figure 8.

### 5 Elementary excitations

In the present section, we discuss the nature of the elementary excitations in the various gapped phases of the quarter-filled two leg ladder. Due to the spin-charge separation, all of the insulating phases have charge excitations of charge  $\pm e$  and zero spin. However, the nature of the magnetic excitations is dependent of the nature of the phases considered. Below, we review the various phases with their elementary excitations.

#### 5.1 $(\pi, \pi)$ -CDW and $(\pi, 0)$ -BOW

##### 5.1.1 Charge excitations

In these two phases,  $y_3 \rightarrow +\infty$ , implying that the effective Hamiltonian for the charge sector is described by two sine-Gordon Hamiltonians:

$$H_{\text{eff}}^c = H_+^c + H_-^c, \quad (61)$$

where

$$H_{\alpha}^c = \int \frac{dx}{2\pi} \left[ u_{\rho\alpha} K_{\rho\alpha} (\pi \Pi_{\rho\alpha})^2 + \frac{u_{\rho\alpha}}{K_{\rho\alpha}} (\partial_x \phi_{\rho\alpha})^2 \right] + \frac{2g_{\alpha}}{(2\pi a)^2} \int dx \cos 4\phi_{\rho\alpha}, \quad (62)$$

$\alpha = \pm$ . Thus, the elementary excitations can be described in terms of solitons of two decoupled sine-Gordon models. Following a semiclassical argument, a soliton is joining two consecutive minima of the Hamiltonian (62). These

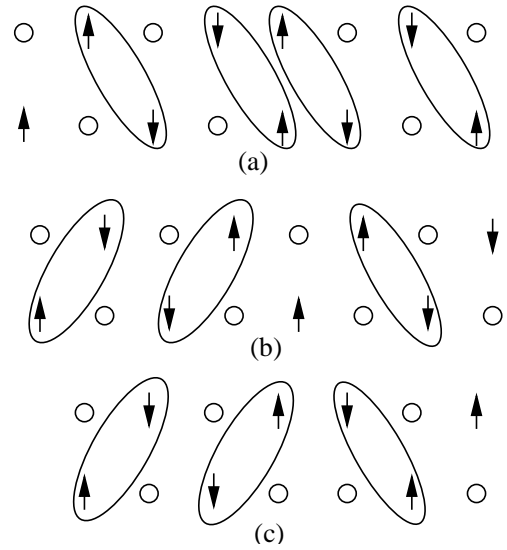


**Fig. 9.** Excitations of the quarter filled ladder in the zig-zag charge ordered phase: (a) Charged excitation: it can be viewed as a domain wall between the two zig-zag charge ordered ground states of the ladder or equivalently as a bound state of two antiholons of the quarter-filled chains. (b) spinon excitation. It can be viewed as a domain wall on the spontaneously dimerized effective zig-zag ladder or as spinon inside one of the chains. (c) Neutral excitations. It can be viewed either as a domain wall between the two zig-zag charge ordered ground states or as a holon-antiholon bound state.

minima are given by  $\langle \phi_{\rho\alpha} \rangle \equiv \pi/4[\pi/2]$ . As a result, the charge of solitons is given by:

$$q_{\alpha} = -\frac{2}{\pi} \int_{-\infty}^{+\infty} \partial_x \phi_{\rho\alpha} = -\frac{2}{\pi} [\phi_{\rho\alpha}(+\infty) - \phi_{\rho\alpha}(-\infty)] = \pm 1. \quad (63)$$

These solitons can be understood as domain walls between the two charge ordered ground states as represented in Figure 9a and Figure 9c. Alternatively, the charged solitons can be viewed as holon-holon (for charge  $-e$ ) or antiholon-antiholon (for charge  $+e$ ) bound states. The neutral solitons can similarly be viewed as holon-antiholon bound state. An immediate consequence of the mapping of the charge excitations onto the sine-Gordon model is that the transport properties of the quarter-filled ladder can be obtained from the methods reviewed in reference [61]. For  $K_{\rho\alpha} > 1/4$ , the solitons are the only possible excitations in the model. For more strongly repulsive excitations, the formation of soliton bound states (breathers) becomes possible. The existence of these excitations translates into an exciton peak in the optical conductivity. Such exciton peak has been studied in the case of the single Hubbard chain in reference [78]. However, in the model we are considering, for  $K_{\rho\alpha} < 1/4$ , intrachain Umklapp scattering becomes relevant and total/antisymmetric charge excitations do not decouple anymore in this regime.

### 5.1.2 Spin excitations

To describe spin excitations, we need to consider the effective Hamiltonian of the spin modes:

$$H_\sigma = \int \frac{dx}{2\pi} \sum_{r=\pm} \left[ u_{\sigma,r} K_{\sigma,r} (\pi \Pi_{\sigma,r})^2 + \frac{u_{\sigma,r}}{K_{\sigma,r}} (\partial_x \phi_{\sigma,r})^2 \right] + \frac{2g_2}{(2\pi\alpha)^2} \int dx \cos 2\phi_{\sigma+} \cos 2\theta_{\sigma-}. \quad (64)$$

This Hamiltonian corresponds exactly to the bosonized Hamiltonian of a zig-zag spin ladder [79–81]. Remarkably, in the strong coupling limit  $V_\parallel, V_\perp, U \gg t_\perp, t$ , a mapping on a zig-zag spin chain was derived to describe the low energy excitations in the  $(\pi, \pi)$ -CDW phase [48]. We thus notice the continuity between the weak coupling and the strong coupling limit for the spin excitations of the  $(\pi, \pi)$ -CDW in this problem. Spin excitations of the quarter filled ladder are those of a zig-zag ladder, *i.e.* massive spinons. A more detailed picture of the spin excitations can be gained by applying a transformation due to Witten and Shankar [81–83]. We first notice that we have  $K_{\sigma+} K_{\sigma-} = 1$  and  $u_{\sigma+} = u_{\sigma-}$ . Thus, we can perform a duality transformation  $\tilde{\phi}_{\sigma-} = \theta_{\sigma-}, \tilde{\theta}_{\sigma-} = \phi_{\sigma-}$ , and introduce:

$$\phi_a = \frac{\phi_{\sigma+} + \tilde{\phi}_{\sigma-}}{\sqrt{2}} \quad (65)$$

$$\phi_b = \frac{\phi_{\sigma+} - \tilde{\phi}_{\sigma-}}{\sqrt{2}}. \quad (66)$$

This procedure permits us to reduce the effective Hamiltonian to:

$$H = H_a + H_b \quad (67)$$

$$H_a = \int \frac{dx}{2\pi} \left[ u_a K_a (\pi \Pi_a)^2 + \frac{u_a}{K_a} (\partial_x \phi_a)^2 \right] - \frac{g_2}{(2\pi\alpha)^2} \int dx \cos \sqrt{8}\phi_a \quad (68)$$

$$H_b = \int \frac{dx}{2\pi} \left[ u_b K_b (\pi \Pi_b)^2 + \frac{u_b}{K_b} (\partial_x \phi_b)^2 \right] - \frac{g_2}{(2\pi\alpha)^2} \int dx \cos \sqrt{8}\phi_b, \quad (69)$$

where  $u_a = u_b = u_{\sigma+}$ ,  $K_a = K_b = K_{\sigma+}$  and  $g_2$  preserves  $SU(2)$  symmetry. The original Hamiltonian (64) is thus decoupled into two massive sine-Gordon model at the  $SU(2)$  point. They describe two massive spin excitations carrying spin 1/2. In the strong coupling limit, the spin excitations can be viewed as the spinons of a zig-zag ladder (see Fig. 9).

### 5.2 $(\frac{\pi}{2}, \frac{\pi}{2})$ -CDW

In the  $(\frac{\pi}{2}, \pm\frac{\pi}{2})$ -charge density wave phases, the charge excitations carry the same quantum numbers as in the

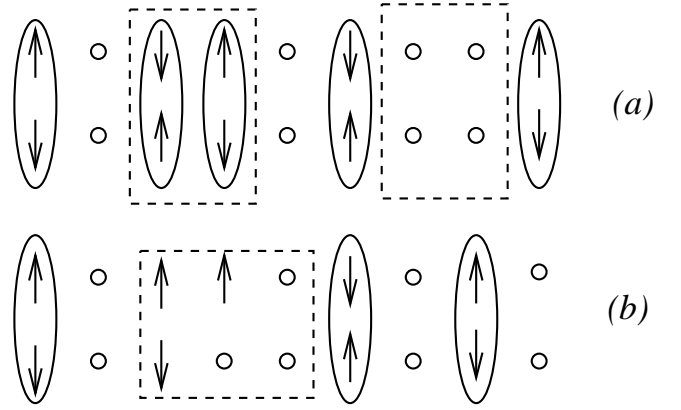


**Fig. 10.** Elementary excitations in the  $(\pi, 0)$ -CDW. Dotted boxes have been drawn to emphasize the location of these excitations along the ladder. (a) holon and antiholon excitations carrying the charge  $\pm e$  respectively. (b) Mixed spin/orbital excitation.

zig-zag charge ordered phase. They correspond to domain walls between the four different  $(\frac{\pi}{2}, \frac{\pi}{2})$ -CDW ground states. However, spin excitations are of a different nature since both  $S_1^z$  and  $S_2^z$  are good quantum numbers. In fact, these spin excitations are massive spinons “confined” within each chain.

### 5.3 phases with $\langle \phi_{\rho-} \rangle = \frac{\pi}{2}$

The total charge excitations still carry  $\pm e$ , as in the previous phase, but this time it is not possible to decouple spin excitations from antisymmetric charge excitations. When  $\phi_{\sigma-}$  is ordered, we have  $\phi_{\rho-}(+\infty) - \phi_{\rho-}(-\infty) = \pm\pi/2$ ,  $\phi_{\sigma+}(+\infty) - \phi_{\sigma+}(-\infty) = \pm\pi/2$  and  $\phi_{\sigma-}(+\infty) - \phi_{\sigma-}(-\infty) = \pm\pi/2$ . As a result, the elementary excitations carry total charge zero, charge difference  $\pm e$ , and spin  $S_1^z = \pm 1/2$  or  $S_2^z = \pm 1/2$ . These elementary excitations can be viewed as a three body bound state of a holon in one chain, an antiholon in the other chain and a spinon. This excitation is sketched in Figure 10.

In fact, there exists an interesting analogy between the spin/antisymmetric charge sector of the quarter filled ladder and the half-filled Hubbard-Kondo-Heisenberg (HKH) chain.

The half-filled HKH chain is described by the Hamiltonian:

$$H = -t \sum_{i,\sigma} (c_{i+1,\sigma}^\dagger c_{i,\sigma} + c_{i,\sigma}^\dagger c_{i+1,\sigma}) + U \sum_i n_{i,\uparrow} n_{i,\downarrow} + \frac{J_K}{2} \sum_{i,\alpha,\beta} \mathbf{S}_i \cdot c_{i,\alpha}^\dagger \boldsymbol{\sigma}_{\alpha,\beta} c_{i,\beta} + J_H \sum_i \mathbf{S}_i \cdot \mathbf{S}_{i+1}, \quad (70)$$

where  $\sigma^{x,y,z}$  are the usual Pauli matrices. At half-filling, the resulting bosonized Hamiltonian [84–86] reads:

$$\begin{aligned}
H = & \int \frac{dx}{2\pi} \left[ u_\rho K_\rho (\pi \Pi_\rho)^2 + \frac{u_\rho}{K_\rho} (\partial_x \phi_\rho)^2 \right] \\
& + \int \frac{dx}{2\pi} \left[ u_{\sigma+} K_{\sigma+} (\pi \Pi_{\sigma+})^2 + \frac{u_{\sigma+}}{K_{\sigma+}} (\partial_x \phi_{\sigma+})^2 \right] \\
& + \int \frac{dx}{2\pi} \left[ u_{\sigma-} K_{\sigma-} (\pi \Pi_{\sigma-})^2 + \frac{u_{\sigma-}}{K_{\sigma-}} (\partial_x \phi_{\sigma-})^2 \right] \\
& + \frac{2J_K}{(2\pi a)^2} \int dx \cos \sqrt{2} \phi_\rho [\cos 2\phi_{\sigma-} - \cos 2\phi_{\sigma+} \\
& + 2 \cos 2\theta_{\sigma-}]. \tag{71}
\end{aligned}$$

Making a rescaling  $\phi_\rho = \sqrt{2} \phi_{\rho-}$ ,  $K_\rho = 2K_{\rho-}$ , we obtain the same Hamiltonian as the one describing the spin/charge difference excitations of the quarter-filled ladder (22–27). In particular, the point  $K_{\rho-} = 1/2$  in the quarter filled ladder corresponds to  $K_\rho = 1$  in the Kondo-Heisenberg chain, *i.e.*  $U = 0$  in (70). Thus, magnetic properties near the metal insulator transition of the quarter filled ladder should be analogous to those of a Kondo-Heisenberg insulator. Close to  $K_{\rho-} = 1$ , the structure of excitations is quite different. In the vicinity of that point [87], gapful excitations of the ladder away from half-filling are described by a massive  $SO(3) \times SO(3)$  Gross-Neveu model [88] as a consequence of the breaking of the original  $SU(4)$  symmetry to  $SU(2) \times SU(2)$ . The enhancement of the symmetry by the RG is instead absent for  $K_{\rho-} = 1/2$ .

## 6 Numerical study of the phase diagram

In this section we discuss the numerical results of the RG equations. Prior than that we analyze in details the nature of the transition among the various phases. The analysis is partially accomplished by a mapping onto a Majorana fermion theory, that gives also rise to a connection with the spin-orbital models.

### 6.1 Mapping on a theory containing Majorana Fermions

We consider first the part of the Hamiltonian (27) with couplings  $g_{4,5,6}$ . It is convenient to rewrite this part of the interaction in terms of massive Majorana fermion operators  $\xi_\nu$  ( $\nu = 0, 1, 2, 3$ ). Using the identities [89]:

$$\frac{\cos 2\phi_{\sigma+}}{\pi a} = i(\zeta_{R,1}\zeta_{L,1} + \zeta_{R,2}\zeta_{L,2}), \tag{72}$$

$$\frac{\cos 2\phi_{\sigma-}}{\pi a} = i(\zeta_{R,3}\zeta_{L,3} + \zeta_{R,0}\zeta_{L,0}), \tag{73}$$

$$\frac{\cos 2\theta_{\sigma-}}{\pi a} = i(\zeta_{R,0}\zeta_{L,0} - \zeta_{R,3}\zeta_{L,3}), \tag{74}$$

and the relation  $g_5 = g_4 + g_6$ , the interaction terms  $g_{4,5,6}$  are rewritten as:

$$\begin{aligned}
i \cos 2\phi_{\rho-} \left[ \frac{g_4}{2\pi a} (\zeta_{R,1}\zeta_{L,1} + \zeta_{R,2}\zeta_{L,2} + \zeta_{R,3}\zeta_{L,3}) \right. \\
\left. + \frac{g_5 + g_6}{2\pi a} \zeta_{R,0}\zeta_{L,0} \right], \tag{75}
\end{aligned}$$

where  $g_5 + g_6$  is always a positive quantity.

In the continuum limit, following reference [89] we can express the bosonic exponents in terms of the order ( $\sigma_i$ ) and disorder ( $\mu_i$ ) parameters of four Ising models as follows:

$$\cos \phi_{\sigma+} = \sigma_1 \sigma_2, \tag{76}$$

$$\cos \phi_{\sigma-} = \sigma_3 \sigma_0, \tag{77}$$

$$\sin \phi_{\sigma+} = \mu_1 \mu_2, \tag{78}$$

$$\cos \theta_{\sigma-} = \mu_3 \sigma_0. \tag{79}$$

When  $\langle \phi_{\rho-} \rangle = \frac{\pi}{2}$ , the Ising order parameter  $\sigma_0$  has a non-zero expectation value. However the sign of  $g_4$  is not fixed. For  $g_4 > 0$ , and  $\langle \phi_{\rho-} \rangle = \frac{\pi}{2}$ ,  $\sigma_{1,2,3}$  have all nonzero expectation values, corresponding to have both  $\phi_{\sigma+}$  and  $\phi_{\sigma-}$  ordered. For  $g_4 < 0$ ,  $\mu_{1,2,3}$  have all nonzero expectation values, corresponding to having both  $\phi_{\sigma+}$  and  $\theta_{\sigma-}$  ordered.

Now, we would like to focus on the interaction part of the Hamiltonian that contains the terms  $g_1, g_2, g_{\sigma\pm}$ . Using the mapping on Majorana fermions, we can write this part as:

$$\begin{aligned}
\frac{g_{\sigma+}}{2\pi^2} (\partial_x \phi_{\sigma+})^2 + \frac{g_{\sigma-}}{2\pi^2} (\partial_x \phi_{\sigma+})^2 + \frac{g_1}{2(\pi a)^2} \cos 2\phi_{\sigma-} \cos 2\phi_{\sigma+} \\
+ \frac{g_2}{2(\pi a)^2} \cos 2\theta_{\sigma-} \cos 2\phi_{\sigma+} = \\
- g_{\sigma+} \zeta_{R,1} \zeta_{L,1} \zeta_{R,2} \zeta_{L,2} - g_{\sigma-} \zeta_{R,0} \zeta_{L,0} \zeta_{R,3} \zeta_{L,3} \\
- g_+ (\zeta_{R,1} \zeta_{L,1} + \zeta_{R,2} \zeta_{L,2}) \zeta_{R,0} \zeta_{L,0} \\
- g_- (\zeta_{R,1} \zeta_{L,1} + \zeta_{R,2} \zeta_{L,2}) \zeta_{R,3} \zeta_{L,3}. \tag{80}
\end{aligned}$$

where  $g_\pm = (g_1 \pm g_2)/2$ . Using the  $SU(2)$  symmetry conditions(44), this expression can be further rewritten as:

$$\begin{aligned}
- g_{\sigma+} (\zeta_{R,1} \zeta_{L,1} \zeta_{R,2} \zeta_{L,2} + \zeta_{R,1} \zeta_{L,1} \zeta_{R,3} \zeta_{L,3} \\
+ \zeta_{R,2} \zeta_{L,2} \zeta_{R,3} \zeta_{L,3}) \\
- g_{\sigma-} (\zeta_{R,1} \zeta_{L,1} + \zeta_{R,2} \zeta_{L,2} + \zeta_{R,3} \zeta_{L,3}) \zeta_{R,0} \zeta_{L,0}, \tag{81}
\end{aligned}$$

which makes the  $SU(2)$  symmetry transparent. We note that for  $g_{\sigma-} > 0$ ,  $i\langle \zeta_{R,a} \zeta_{L,a} \rangle$  can have opposite signs depending whether  $a = 0$  or  $a \neq 0$ . This implies that either  $\langle \mu_0 \rangle \neq 0$  and  $\langle \sigma_{1,2,3} \rangle \neq 0$  or  $\langle \sigma_0 \rangle \neq 0$  and  $\langle \mu_{1,2,3} \rangle \neq 0$ . Both cases correspond to having  $\theta_{\sigma-}$  and  $\phi_{\sigma+}$  ordered. When  $g_{\sigma-} < 0$ , we have both  $\phi_{\sigma+}$  and  $\phi_{\sigma-}$  ordered.

#### 6.1.1 Spin-orbital models

Before closing this section, we would like to discuss the following connection. If we consider the case of  $V_{\parallel} = 0$ ,

$J_{\perp} = 0$  and  $V_{\perp} = U$ , we can rewrite the interchain interaction in equation (1) as:

$$\frac{U}{2} \sum_i (n_{i,1,\uparrow} + n_{i,1,\downarrow} + n_{i,2,\uparrow} + n_{i,2,\downarrow})^2, \quad (82)$$

which has a manifest  $SU(4)$  invariance. Thus the problem is related to the quarter-filled  $SU(4)$  Hubbard model [90]. The charge Umklapp term derived for that model [90] agrees with (23). If  $U$  is large enough, the low energy excitations are those of an antiferromagnetic chain of  $SU(4)$  spins [90]. Considering deviations from the  $SU(4)$  symmetric point, it is possible to derive a model describing the low energy excitations of the insulator [41] in terms of coupled spin and orbital modes (the spin-orbital model). In references [88,91,92], a  $SU(2) \times SU(2)$  spin-orbital symmetric model was analyzed perturbatively around the  $SU(4)$  point using bosonization and refermionization techniques. An Hamiltonian describing the low energy dynamics of the system with six Majorana fermions was obtained, and the formation of a dimerized spin gapped phase was predicted in the physical range of parameters. The existence of this dimerized phase was also confirmed by numerical studies [92,93]. In our present problem, assuming  $K_{\rho-} \sim 1$  so that the term containing  $g_3$  can be neglected, and using the mapping:

$$\frac{\cos 2\phi_{\rho-}}{\pi a} = i(\zeta_{R,4}\zeta_{L,4} + \zeta_{R,4}\zeta_{L,4}), \quad (83)$$

we can recast the interactions in the spin/antisymmetric charge sector of equation (27) in terms of two triplets of Majorana fermions:  $(\zeta_1, \zeta_2, \zeta_3)$  representing the spin excitations, and  $(\zeta_0, \zeta_4, \zeta_5)$  representing the orbital excitations as in references [88,91,92]. The Hamiltonian we obtain is however more general, since we did not assume any  $SU(2)$  symmetry in the orbital sector. From our previous discussion of the phase diagram in Section 4 we expect that the dimerized phase (Phase IV in Ref. [92] or Phase A in Ref. [91]) of the spin-orbital model is related to the  $(\pi, 0)$ -BOW. In a different limit [94,95] of the  $SU(2) \times SU(2)$  spin-orbital model, a dimerized insulating phase analogous to the  $(\pi, 0)$ -BOW was also obtained. We note that no charge ordering is predicted by the  $SU(2) \times SU(2)$  spin orbital model. The reason for this is that the  $V_{\parallel}$  term of the ladder model produces a large renormalization of  $K_{\rho-}$  in the charge ordered state, while leaving  $K_{\sigma-}, K_{\sigma+}$  close to the non-interacting value, due to the remaining  $SU(2)$  symmetry. To describe charge ordering, one has thus to consider more general spin-orbital models in which the interaction in the orbital sector has only the  $U(1)$  symmetry [41].

## 6.2 Order of the transitions between the different phases

We now turn to the quantum phase transitions between the different phases of the quarter-filled ladder. These phase transitions can result from a change of the ordering

in the  $\phi_{\rho-}$  field, the spin gap being preserved, or from a change of the ordering in the spin sector. As we will see below, the former phase transitions are of second order and belong to the one-dimensional quantum Ising universality class, whereas the latter transitions can be either of second and first order. We begin discussing the Ising transitions in the antisymmetric charge mode.

### 6.2.1 Ising transitions

We consider phase transitions in which the order in the spin sector is not changed, but the order in the antisymmetric charge sector  $\phi_{\rho-}$  is modified. These transitions occur between the  $(\pi, 0)$ -BOW and the  $(\pi, \pi)$ -CDW, the  $(\frac{\pi}{2}, \pi)$ -CDWs and the  $(\frac{\pi}{2}, \frac{\pi}{2})$ -CDWs, the  $(\pi, \pi)$ -BOW and the  $(\pi, 0)$ -CDW. Since the order in the spin sector does not change we can describe the transition by concentrating only on the  $\phi_{\rho-}$  modes. The resulting effective Hamiltonian reads:

$$H_{\rho-} = \int \frac{dx}{2\pi} \left[ u_{\rho-} K_{\rho-} (\pi \Pi_{\rho-})^2 + \frac{u_{\rho-}}{K_{\rho-}} (\partial_x \phi_{\rho-})^2 \right] + \frac{2g_3}{(2\pi a)^2} \int dx \cos 4\phi_{\rho-} + \frac{2\bar{g}}{(2\pi a)^2} \int dx \cos 2\phi_{\rho-}. \quad (84)$$

This Hamiltonian is the one of the double sine-Gordon model [96]. The semiclassical analysis of the double cosine potential shows that for  $\langle \phi_{\rho-} \rangle = \pm \frac{\pi}{4}$ ,  $\langle \cos 2\phi_{\rho-} \rangle = 0$ . Using the result of [96], this implies that as  $\bar{g}$  is varied, an Ising transition is obtained in  $\phi_{\rho-}$ . For the sake of simplicity, let us consider the transition between the  $(\pi, 0)$ -BOW and the  $(\pi, \pi)$ -CDW. Similar features appear in all the other Ising transitions. In the  $(\pi, \pi)$ -CDW, the order parameter  $O_{\text{CDW}(\pi,\pi)} \sim \sin 2\phi_{\rho-}$ . Using the results of [96] on the ultraviolet-infrared transmutation of operators, it is easily seen that  $O_{\text{CDW}(\pi,\pi)} \sim \mu$ , where  $\mu$  is the disorder parameter of a quantum Ising model. This implies in particular that  $\langle O_{\text{CDW}(\pi,\pi)}(x) O_{\text{CDW}(\pi,\pi)}(0) \rangle \sim x^{-1/4}$  at the transition. Moreover, near the transition one has:

$\langle O_{\text{CDW}(\pi,\pi)} \rangle \sim \left( \frac{a\Delta_{\rho-}}{v} \right)^{1/8}$ . If the gap  $\Delta_{\rho-}$  vanishes linearly with the interaction  $V$  this implies  $\langle O_{\text{CDW}(\pi,\pi)} \rangle \sim (V - V_c)^{1/8}$ , giving rise to the onset of the order parameter at a critical value  $V_c$ . Such onset was numerically observed at the homogeneous insulator  $\text{HI}_{sg}$ - $\text{CDW}_{sg}$  transition in reference [48] and attributed to an Ising transition.

A simple picture of the transition is obtained, in the limit of strong coupling  $V_{\perp} \rightarrow \infty$ , by an effective quantum Ising model. In this picture, the only states retained are the electron pairs forming singlets along the diagonal and pointing either in the northwest or northeast direction. The variable  $\sigma^z = 1$  when the diagonal singlet formed of two electrons is oriented northwest (NW), and  $\sigma^z = -1$  when the singlet is oriented northeast (NE). In the ground state all the electron pairs must have the same orientation. The corresponding potential energy reads:

$$H_{\text{pot.}} = -V_{\parallel} \sum_n \sigma_n^z \sigma_{n+1}^z. \quad (85)$$

The kinetic energy comes from the term  $t$ . In second order perturbation theory,  $t$  flips a singlet pair from the NW to NE orientation. This process leads to a kinetic term in the Hamiltonian:

$$H_{kin.} = \frac{t_{\parallel}^2}{V_{\perp}} \sigma_n^x. \quad (86)$$

When the kinetic term in the Hamiltonian dominates, the singlet pairs go back and forth between NE and NW orientation leading to a zero average of the  $(\pi, \pi)$ -CDW order parameter, and an effective bond order wave. When the potential energy dominates, the singlet pairs are all locked in the NE or NW orientation giving rise to a nonzero  $(\pi, \pi)$ -CDW.

### 6.2.2 Spin transitions

In the present section, we discuss the transitions in the spin sector. Since the gaps in the  $\phi_{\rho-}$  and  $\phi_{\rho+}$  sectors are robust, we can concentrate on a low energy effective spin model. First, let us focus on the case of  $\langle \phi_{\rho-} \rangle = \frac{\pi}{2}$ . In that case, the discussion is equivalent to the one in reference [52]. The theory describing the transition point is the  $O(3)$  Gross-Neveu model, and the operator that takes the system away from the transition point is the mass of the Gross-Neveu fermions. As a result, the system will have a second order phase transition in the  $SU(2)_2$  WZW model universality class when the  $O(3)$  Gross-Neveu has no spontaneous symmetry breaking and a first order transition when the Gross-Neveu model presents dynamical mass generation [97,98]. For  $g_{\sigma+} < 0$ , there is a spontaneous symmetry breaking and thus a first order transition. Since this corresponds to  $J_{\perp} > 0$ , first order spin transitions should be generic in the models we are considering. In particular, first order transitions should be expected between phases such as the  $(\pi, 0)$ -BOW and the  $(\frac{\pi}{2}, \pi)$ -CDW or the  $(\pi, 0)$ -CDW and the  $(\frac{\pi}{2}, \pi)$ -CDW. These first order transitions occur in the spin sector and should be observable by looking at spin-spin correlations. In the case of  $\langle \phi_{\rho-} \rangle = \frac{\pi}{4}$ , we have to focus on the terms coming from  $g_1, g_2, g_{\sigma\pm}$ . In that case, for a transition to be possible we must have  $g_{\sigma-} = 0$  as one can see directly from equation (80). The behavior at the transition then depends on the sign of  $g_{\sigma+}$ . When  $g_{\sigma+} > 0$ , no gap is generated in the triplet modes thus giving a  $SU(2)_1 \times SU(2)_1$  criticality. For  $g_{\sigma+} < 0$ , the triplet modes remain massive at the transition, leading to an Ising criticality. Since  $g_{\sigma+} \sim -J_{\perp} < 0$ , an Ising transition is obtained between the  $(\pi, \pi)$ -BOW and the  $(\frac{\pi}{2}, \frac{\pi}{2})$ -CDW or the  $(\pi, \pi)$ -CDW and the  $(\frac{\pi}{2}, \frac{\pi}{2})$ -CDW.

### 6.3 RG calculation

To find the phase diagram, we integrate the equations (47) numerically using a fourth order Runge-Kutta algorithm for fixed values of  $K_{\rho-}$  at varying  $V_{\perp}$  and  $J_{\perp}$ . We stop the numerical integration when one of the coupling constants  $y_3, y_5, y_6$  becomes of order 1. We find that at this scale,

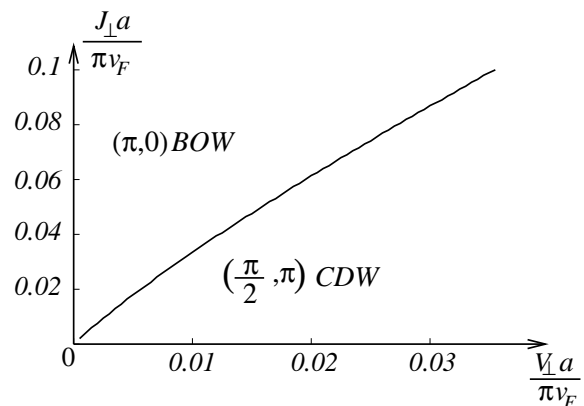


**Fig. 11.** The topology of the phase diagram of the quarter filled ladder for  $K_{\rho-} \lesssim 1/2$ . Only the  $(\pi, 0)$ -BOW and the  $(\frac{\pi}{2}, \pi)$ -CDW are obtained.

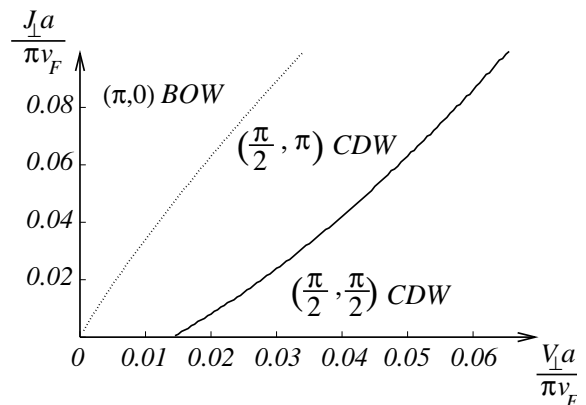


**Fig. 12.** The topology of the phase diagram of the quarter filled ladder for  $1/2 > K_{\rho-} \gtrsim 1/3$ . The  $(\frac{\pi}{2}, \frac{\pi}{2})$ -CDW appears at large  $V_{\perp}$ .

$|y_1|, y_2$  are still inferior to 1. We have the following results. First, for  $K_{\rho-}$  larger than  $1/3$ , ( $K_{\rho-} \simeq 1/2$ ) the  $(\frac{\pi}{2}, \frac{\pi}{2})$ -CDW and  $(\pi, \pi)$ -CDW are absent. This is a consequence of the fact that in this regime, the  $2k_F$  fluctuations are dominant over the  $4k_F$  ones. As a result, we find either the bond order wave  $(\pi, 0)$ -BOW or the  $(\frac{\pi}{2}, \pi)$ -CDW. As could be expected, a large  $J_{\perp}$  favors the former, and a large  $V_{\perp}$  favors the latter. A first order transition is expected between these two phases. The phase diagram for  $K_{\rho-} = 0.5$  is drawn in Figure 11. When  $K_{\rho-}$  becomes smaller but still larger than  $1/3$ , the term  $\cos 4\phi_{\rho-}$  is more relevant and the  $(\frac{\pi}{2}, \frac{\pi}{2})$ -CDW phase becomes stable at large  $V_{\perp}$ . This can be understood as resulting from an increase in the strength of  $4k_F$  fluctuations. The phase diagram for  $K_{\rho-} = 0.35$  is sketched in Figure 12. For  $K_{\rho-}$  close to  $1/3$ , the topology of the phase diagram becomes more complex. The  $(\pi, \pi)$ -CDW phase is present for competing  $V_{\perp}, J_{\perp}$ , along with the  $(\pi, 0)$ -BOW and the two other CDWs. The phase diagram is sketched in Figure 13. Finally, for  $K_{\rho-} < 1/3$ ,  $\cos 4\phi_{\rho-}$  is the most relevant operator, and the  $(\frac{\pi}{2}, \pi)$ -CDW phase disappears altogether. The  $(\pi, \pi)$ -CDW phase

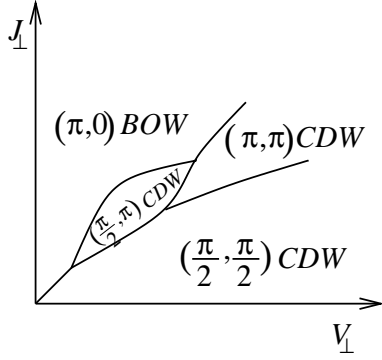


**Fig. 13.** The topology of the phase diagram of the quarter filled ladder for  $K_{\rho-} \lesssim 1/3$ . The size of the  $(\frac{\pi}{2}, \pi)$ -CDW phase region has been exaggerated.

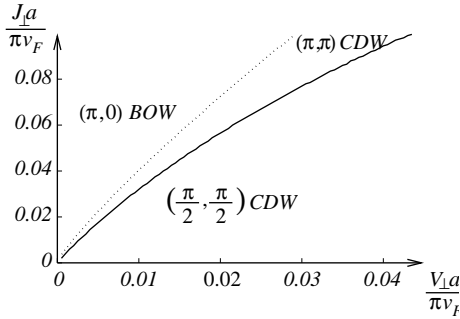


**Fig. 14.** The topology of the phase diagram of the quarter filled ladder for  $K_{\rho-} < 1/3$ . The  $(\pi, 0)$ -BOW is obtained for strong  $J_{\perp}$  and the  $(\frac{\pi}{2}, \frac{\pi}{2})$ -CDW is obtained for strong  $V_{\perp}$ . The  $(\pi, \pi)$ -CDW is obtained in the intermediate regime.

is obtained for  $V_{\perp}, J_{\perp}$  intermediate, whereas for strong  $J_{\perp}$ , the  $(\pi, 0)$ -BOW is obtained and for strong  $V_{\perp}$ , the  $(\frac{\pi}{2}, \frac{\pi}{2})$ -CDW is obtained. The phase diagram for  $K_{\rho-} = 0.3$  is sketched in Figure 14.

## 6.4 Commensurate-incommensurate transitions

### 6.4.1 Deviations from quarter filling

Away from quarter filling, the number of particles is fixed *via* a chemical potential that affects only  $H_{\rho+}$ . The charge modes are described by the Hamiltonian:

$$H_{\rho+} = \int \frac{dx}{2\pi} \left[ u_{\rho+} K_{\rho+} (\pi \Pi_{\rho+})^2 + \frac{u_{\rho+}}{K_{\rho+}} (\partial_x \phi_{\rho+})^2 \right] - \frac{2\mu}{\pi} \int dx \partial_x \phi_{\rho+} - \frac{2V_{\perp} a}{(2\pi a)^2} \int dx \cos 4\phi_{\rho+} \quad (87)$$

where  $\mu$  measures the difference in chemical potential. A standard argument [99–101] then shows that for a difference in chemical potential of the order of the gap of the quarter filled system, a commensurate-incommensurate (C-I) transition occurs and the system becomes gapless. The renormalized  $K_{\rho+}^*$  exponent at the gapless point is

such [101] that the dimension of the operator  $\cos 4\phi_{\rho+}$  is one, which gives  $K_{\rho+}^* = 1/4$ . This result has been previously derived from different arguments in reference [19] and checked against numerical simulations.

In the incommensurate phase, the  $\frac{\pi}{2}$ -CDW correlations are the dominant ones as they behave as  $\langle e^{i\phi_{\rho+}(x)} e^{-i\phi_{\rho+}(0)} \rangle \sim x^{-K_{\rho+}/2}$ . Subdominant  $\pi$ -BOW or  $\pi$ -CDW correlations are also present and behave as  $\langle e^{i2\phi_{\rho+}(x)} e^{-i2\phi_{\rho+}(0)} \rangle \sim x^{-2K_{\rho+}}$ . Right at the transition, the respective exponents are  $1/8$  and  $1/2$ .

In principle, superconducting correlations are also possible. The only surviving superconducting order parameter is the *d*-wave one. Its lattice expression is given by:

$$O_{SC}^d(i) = \sum_{\sigma} (c_{i,1,\sigma} c_{i,2,-\sigma} - c_{i,2,\sigma} c_{i,1,-\sigma}). \quad (88)$$

One finds that this pairing operator behaves as  $\langle e^{i\theta_{\rho+}(x)} e^{-i\theta_{\rho+}(0)} \rangle \sim x^{-1/(2K_{\rho+})}$ . Right at the C-I transition, these correlations have an exponent 2 which indicates that superconductivity is largely dominated by CDW correlations. In a doped quarter filled insulator the presence of the spin gap is therefore insufficient to render superconducting correlations dominant. This is to be contrasted with the case of the half-filled ladder [102] where superconducting correlations are dominant in the conducting phase.

### 6.4.2 Effect of a magnetic field

An applied magnetic field couples to the ladder *via* a term:

$$H_{\text{mag.}} = -\frac{h}{\pi} \int dx \partial_x \phi_{\sigma+}. \quad (89)$$

It is well known that a magnetic field applied to a spin gap system can produce a Luttinger liquid like phase [103] when the field becomes larger than the gap. The effect of the magnetic field is different in the case of strong repulsion ( $\langle \phi_{\rho-} \rangle = \frac{\pi}{4}$ ) and in the case of weaker repulsion ( $\langle \phi_{\rho-} \rangle = \frac{\pi}{2}$ ). For strong repulsion the spin-gap is caused by the terms  $g_1$  or  $g_2$ . The effect of the applied field is to render these two terms irrelevant. As a result, both  $\phi_{\sigma+}$  and  $\phi_{\sigma-}$  have gapless excitations leading to a C0S2 phase in the notations of reference [31]. This C0S2 phase contains in chain  $2k_F$  charge density and spin-density wave power-law correlations. One finds in the case of C0S2 phase obtained by applying a magnetic field to the  $(\pi, \pi)$ -CDW or the  $(\pi, \pi)$ -BOW:

$$\langle O_{\text{CDW}_{2k_F,p}}(x) O_{\text{CDW}_{2k_F,p}}(0) \rangle \sim \cos\left(\frac{\pi x}{2a}\right) \cos(\pi m x) \frac{\text{const.}}{x^{5/4}}, \quad (90)$$

$$\langle S_p^z(x) S_p^z(0) \rangle \sim \frac{1}{x^2} + \cos\left(\frac{\pi x}{2a}\right) \cos(\pi m x) \frac{\text{const.}}{x^{5/4}}, \quad (91)$$

$$\langle S_p^x(x) S_p^x(0) \rangle \sim \text{const.} \frac{\cos(\pi m x)}{x^{5/2}} + \cos\left(\frac{\pi x}{2a}\right) \frac{\text{const.}}{x^{5/4}}, \quad (92)$$

where exponents have been obtained from the transformation of reference [81] and Section 5.1.2 by requiring that at the transition the dimension of the relevant operators leading to the spin gap in equation (67) be of dimension one [101]. In the case of the COS2 phase obtained by applying a magnetic field to the  $(\frac{\pi}{2}, \frac{\pi}{2})$ -CDWs, one finds instead [103]:

$$\langle O_{\text{CDW}_{2k_F,p}}(x)O_{\text{CDW}_{2k_F,p}}(0) \rangle \sim \cos\left(\frac{\pi x}{2a}\right) \cos(\pi m x) \frac{\text{const.}}{x^{1/2}} \quad (93)$$

$$\langle S_p^z(x)S_p^z(0) \rangle \sim \frac{1}{x^2} + \cos\left(\frac{\pi x}{2a}\right) \cos(\pi m x) \frac{\text{const.}}{x^{1/2}} \quad (94)$$

$$\langle S_p^x(x)S_p^x(0) \rangle \sim \text{const.} \times \frac{\cos(\pi m x)}{x^{5/2}} + \cos\left(\frac{\pi x}{2a}\right) \frac{\text{const.}}{x^2}. \quad (95)$$

For weaker repulsion, the spin gap is caused by the terms  $g_4, g_5, g_6$ . The application of the magnetic field then produces only a suppression of the gap in  $\phi_{\sigma+}$  giving a COS1 phase. The behavior of the induced spin density wave correlations depends on whether  $\phi_{\sigma-}$  or  $\theta_{\sigma-}$  is ordered in the parent case. In the first case, which corresponds to the  $(\frac{\pi}{2}, \pi)$  CDWs under strong magnetic field, critical correlations develop in  $S_p^z(x)$  as well as in the  $(\frac{\pi}{2}, q_y)$ -CDW order parameters with an exponent of 1. In the second case, which corresponds to the  $(\pi, 0)$ -BOW and the  $(\pi, 0)$ -CDW under strong magnetic field, only  $S_p^{x,y}$  become critical with an exponent of  $1/4$ .

## 7 Conclusions

In the present paper, we have studied charge ordering in the two-leg Hubbard ladder at quarter filling. Focusing in the regime of strong-coupling on-site Coulomb repulsion  $U$ , we have investigated the interplay of the interchain Coulomb repulsion  $V_{\perp}$  and the exchange interaction  $J_{\perp}$  on charge ordering, and a variety of spin-gapped charge density waves and bond-order waves have been obtained. In particular, when the intrachain repulsion is strong enough, the ground state of the system exhibits a zig-zag charge order state similar to the phase described in numerical studies [48]. We have obtained the complete phase diagram in the  $J_{\perp} - V_{\perp}$  plane by numerical integration of perturbative renormalization group equations and discussed the transitions between the various charge ordered and bond-ordered states. The results show that phase transitions can occur by an ordering in the antisymmetric charge sector or the spin sectors. The quantum phase transition in the spin sector, as in the half-filled case, is described by the  $O(3)$  Gross-Neveu model [51, 52] with a mass term and can be either second or first order. The transition in the antisymmetric charge sector which is proper to the quarter-filled ladder belongs to the Ising universality class. This

type of Ising transition is expected to separate the zig-zag charge ordered state from a bond ordered wave phase. We have further analyzed the charge and spin excitations in the various gapped phases. Due to charge-spin separation, all of the insulating phases have spinless holon excitations of charge  $\pm e$ . However, the magnetic excitations depend on the nature of the phases considered. For strong intrachain repulsion, they can be either massive spinons confined in each chain in the case of the  $(\frac{\pi}{2}, \frac{\pi}{2})$ -CDWs or domain walls of a dimerized effective zig-zag ladder in the case of a zig-zag charge ordered state in agreement with reference [48]. In the case of weaker intrachain repulsion, we have discussed the analogy of the excitations spin/antisymmetric charge sector of the quarter filled ladder with those of a half-filled Hubbard-Kondo-Heisenberg chain. In the framework of bosonization we have discussed the connection with other effective models of the quarter-filled ladder, such as the spin-orbital models [88, 92]. We have briefly discussed the physics away from quarter filling, where commensurate-incommensurate transitions can occur. The analysis of correlations functions show that CDW correlations largely dominate superconducting fluctuations at odds with half-filled ladders [102]. Finally, we have discussed the effect of magnetic fields strong enough to lift the spin gaps and show that the induced spin density wave correlations sharply distinguish the different charge ordered and bond ordered phases.

We would like to point out that although our results do not directly apply to the  $\text{NaV}_2\text{O}_5$  compound, since in this material  $t_{\perp} = 2t_{\parallel}$ , our model is able to reproduce a zig-zag charge ordered state with spin gap. It would be interesting to compare the features of the zig-zag state we predict with the one obtained in  $\text{NaV}_2\text{O}_5$ . In this perspective, it would be interesting to study in details a model in which interchain hopping is fully taken into account following the approach of [30, 31]. It would also be interesting to extend our analysis to zig-zag ladder models, since experimental realizations of these systems are now available [53].

We thank N. Andrei, M. Cuoco, P. Lecheminant and T. Giamarchi for discussions and comments. E. Orignac acknowledges support from *Ministère de la Recherche et des Nouvelles Technologies* under a grant ‘‘ACI Jeunes chercheurs’’.

## Appendix A: Derivation of the Umklapp term from the lattice Hamiltonian of the quarter-filled ladder

In this appendix, we give a derivation of the  $\cos 4\phi_{\rho+}$  term in the bosonized charge Hamiltonian (23) of the quarter filled ladder following reference [14]. To derive this term, one needs to separate the low energy processes which keep all the particles near the Fermi points  $\pm k_F$  from the high energy processes that involve transfer of particles near the

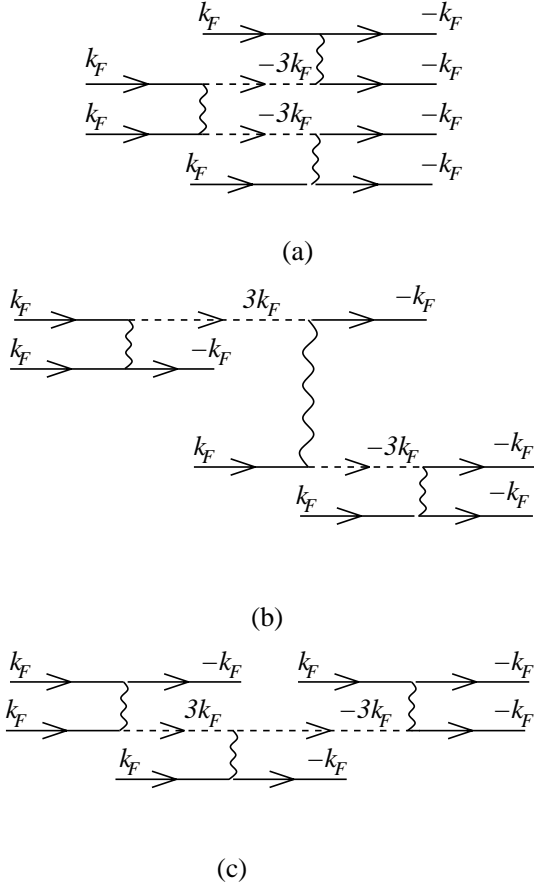


**Fig. 15.** The diagrams that give rise to the  $\cos 4\phi_{\rho+}$  term.

points  $\pm 3k_F$ . By eliminating the latter high energy processes, one is left with an effective action that involve only the Fermi points. The details of the procedure to eliminate the high energy states are exposed in reference [14]. The processes that give rise to the  $\cos 4\phi_{\rho+}$  are represented diagrammatically in Figure 15.

The corresponding terms in the action read for diagram (a):

$$\begin{aligned}
 S_a = & \frac{1}{2L^3} \sum_{r=R,L} \sum_{k_1, k'_1} \sum_{p_1, \sigma_1} \int_0^\beta d\tau_1 \sum_{k_2, k'_2} \sum_{p_2, \sigma_2} \int_0^\beta d\tau_2 \\
 & \times \sum_{k_3, k'_3} \sum_{p_3, \sigma_3} \int_0^\beta d\tau_3 X_{\sigma_1, \sigma'_1}^{p_1, p'_1} X_{\sigma_2, \sigma'_2}^{p_2, p'_2} Y_{\sigma_3, \sigma'_3}^{p_3, p'_3} \\
 & \times \langle (c_{k_1+q_1, -r, p_1, \sigma_1}^\dagger c_{k'_1 - q_1, -r, p'_1, \sigma'_1}^\dagger c_{k'_1, r, p'_1, \sigma'_1} d_{k_1, -r, p_1, \sigma_1})(\tau_1) \\
 & \times (c_{k_2+q_2, -r, p_2, \sigma_2}^\dagger c_{k'_2 - q_2, -r, p'_2, \sigma'_2}^\dagger c_{k'_2, r, p'_2, \sigma'_2} d_{k_2, -r, p_2, \sigma_2})(\tau_2) \\
 & \times (d_{k_3+q_3, -r, p_3, \sigma_3}^\dagger d_{k'_3 - q_3, -r, p'_3, \sigma'_3}^\dagger c_{k'_3, r, p'_3, \sigma'_3} c_{k_3, r, p_3, \sigma_3})(\tau_3) \rangle_d, \quad (96)
 \end{aligned}$$

for diagram (b):

$$\begin{aligned}
 S_b = & \frac{1}{2L^3} \sum_{r=R,L} \sum_{k_1, k'_1} \sum_{p_1, \sigma_1} \int_0^\beta d\tau_1 \sum_{k_2, k'_2} \sum_{p_2, \sigma_2} \int_0^\beta d\tau_2 \\
 & \times \sum_{k_3, k'_3} \sum_{p_3, \sigma_3} \int_0^\beta d\tau_3 X_{\sigma_1, \sigma'_1}^{p_1, p'_1} X_{\sigma_2, \sigma'_2}^{p_2, p'_2} Z_{\sigma_3, \sigma'_3}^{p_3, p'_3} \\
 & \times \langle (d_{k_1+q_1, r, p_1, \sigma_1}^\dagger c_{k'_1 - q_1, -r, p'_1, \sigma'_1}^\dagger c_{k'_1, r, p'_1, \sigma'_1} c_{k_1, r, p_1, \sigma_1})(\tau_1) \\
 & \times (c_{k_2+q_2, -r, p_2, \sigma_2}^\dagger c_{k'_2 - q_2, -r, p'_2, \sigma'_2}^\dagger c_{k'_2, r, p'_2, \sigma'_2} d_{k_2, -r, p_2, \sigma_2})(\tau_2) \\
 & \times (c_{k_3+q_3, -r, p_3, \sigma_3}^\dagger d_{k'_3 - q_3, -r, p'_3, \sigma'_3}^\dagger c_{k'_3, r, p'_3, \sigma'_3} d_{k_3, r, p_3, \sigma_3})(\tau_3) \rangle_d, \quad (97)
 \end{aligned}$$

for diagram (c):

$$\begin{aligned}
 S_c = & \frac{1}{2L^3} \sum_{r=R,L} \sum_{k_1, k'_1} \sum_{p_1, \sigma_1} \int_0^\beta d\tau_1 \sum_{k_2, k'_2} \sum_{p_2, \sigma_2} \int_0^\beta d\tau_2 \\
 & \times \sum_{k_3, k'_3} \sum_{p_3, \sigma_3} \int_0^\beta d\tau_3 X_{\sigma_1, \sigma'_1}^{p_1, p'_1} X_{\sigma_2, \sigma'_2}^{p_2, p'_2} X_{\sigma_3, \sigma'_3}^{p_3, p'_3} \\
 & \times \langle (d_{k_1+q_1, r, p_1, \sigma_1}^\dagger c_{k'_1 - q_1, -r, p'_1, \sigma'_1}^\dagger c_{k'_1, r, p'_1, \sigma'_1} c_{k_1, r, p_1, \sigma_1})(\tau_1) \\
 & \times (c_{k_2+q_2, -r, p_2, \sigma_2}^\dagger c_{k'_2 - q_2, -r, p'_2, \sigma'_2}^\dagger c_{k'_2, r, p'_2, \sigma'_2} d_{k_2, -r, p_2, \sigma_2})(\tau_2) \\
 & \times (c_{k_3+q_3, -r, p_3, \sigma_3}^\dagger d_{k'_3 - q_3, -r, p'_3, \sigma'_3}^\dagger d_{k'_3, -r, p'_3, \sigma'_3} c_{k_3, r, p_3, \sigma_3})(\tau_3) \rangle_d, \quad (98)
 \end{aligned}$$

where we use notations similar to those of reference [14]. The differences with reference [14] are the following. The most important is the apparition of a chain index  $p = 1, 2$  for the fermions. Another difference (very minor) is that we write the annihilation operator for fermions with momentum close to  $k_F$ ,  $c_R$  and  $d_R$  for fermions with momentum close to  $3k_F$ . For fermions with momentum close to  $-k_F$  and  $-3k_F$  we write the respective annihilation operators  $c_L$  and  $d_L$ . We also have by definition  $-R = L$  and  $-L = R$ . We have the following expressions for  $X, Y, Z$ :

$$X_{\sigma\sigma'}^{pp'} = \frac{Ua}{2} \delta_{\sigma, -\sigma'} \delta_{p, p'} + V_\perp a (1 - \delta_{p, p'}) \quad (99)$$

$$Y_{\sigma\sigma'}^{pp'} = (Ua \delta_{\sigma, -\sigma'} - 2V_\parallel) \delta_{p, p'} + V_\perp a (1 - \delta_{p, p'}) \quad (100)$$

$$Z_{\sigma\sigma'}^{pp'} = \left( \frac{Ua}{2} \delta_{\sigma, -\sigma'} - V_\parallel \right) \delta_{p, p'} + V_\perp a (1 - \delta_{p, p'}). \quad (101)$$

The operators  $d_R, d_L$  annihilate states of high energy. In the low energy limit, these states do not appear and should therefore be integrated out [14]. This is the meaning of the symbol  $\langle \dots \rangle_d$ . These states are integrated out by using the following Green's function for the  $d$  fermions:

$$\langle d_{k, r, p, \sigma}(\tau) d_{k', r', p', \sigma'}(0) \rangle = -\frac{1}{2\sqrt{2}t} \delta_{k, k'} \delta_{r, r'} \delta_{p, p'} \delta_{\sigma, \sigma'} \quad (102)$$

where  $t$  is the transfer integral of the extended Hubbard model. This integration gives rise to a term that describes

the collision of four fermions with  $8k_F$  Umklapp. This term reads:

$$S = \frac{1}{8t^2} \int dx A_{\sigma_1 \sigma'_1 \sigma_2 \sigma'_2}^{p_1 p'_1 p_2 p'_2} (\psi_{R,p_1,\sigma_1}^\dagger \psi_{L,p_1,\sigma_1}) (\psi_{R,p'_1,\sigma'_1}^\dagger \psi_{L,p'_1,\sigma'_1}) (\psi_{R,p_2,\sigma_2}^\dagger \psi_{L,p_2,\sigma_2}) (\psi_{R,p'_2,\sigma'_2}^\dagger \psi_{L,p'_2,\sigma'_2}) + \text{h.c.} \quad (103)$$

If all the fermions belong to the same chain ( $p_1 = p'_1 = p_2 = p'_2$ ), one recovers the term  $\cos 4\sqrt{2}\phi_{\rho,p}$  derived in reference [14]. For the case  $(p_1, \sigma_1) = (1, \uparrow)$ ,  $(p'_1, \sigma'_1) = (1, \downarrow)$ ,  $(p_2, \sigma_2) = (2, \uparrow)$ ,  $(p'_2, \sigma'_2) = (2, \downarrow)$  (and all the  $4! = 24$  cases equivalent by permutation), the Umklapp term (103) can be bosonized in the form:

$$S = g \int dx \cos(2(\phi_{1,\uparrow} + \phi_{1,\downarrow} + \phi_{2,\uparrow} + \phi_{2,\downarrow})) = g \int dx \cos 4\phi_{\rho+} \quad (104)$$

This leads to the term we derived phenomenologically. Finding the expression of  $g$  is only a tedious calculation. The final result is:

$$g = \frac{V_\perp(U^2 + 10V_\perp U + 4V_\perp^2 - 4V_\parallel V_\perp)\alpha}{32t^2\pi^2\alpha^2}. \quad (105)$$

## Appendix B: Phenomenological spin density

In this appendix, we give a phenomenological derivation of the  $2nk_F$  Fourier components of the spin density that generalizes the equations (18–20). Let us begin with  $S^z(x)$ . If we have a system of fermions with both spins up and down, we can write the following expression [72] for the spin density:

$$\rho_\alpha(x) = \rho_0 - \frac{1}{\pi} \partial_x \phi_\alpha + \sum_m A_m \cos 2m(\phi_\alpha - k_F x). \quad (106)$$

Expressing these quantities in terms of  $\phi_\rho, \phi_\sigma$ , forming the difference and taking into account the term  $\cos \sqrt{8}\phi_\sigma$  in the Hamiltonian, we obtain the expression:

$$S^z(x) = -\frac{1}{\pi\sqrt{2}} \partial_x \phi_\sigma + \sum_m B_m \sin \sqrt{2}m\phi_\sigma \sin(m\sqrt{2}\phi_\rho - 2k_F x). \quad (107)$$

Since the Hamiltonian of spin excitations contains a term  $\cos \sqrt{8}\phi_\sigma$ , new terms will be generated by fusion of this operator with  $S^z(x)$ . For  $m$  odd, the fusions will generate a term  $\sin \sqrt{2}\phi_\sigma$ . For  $m$  even, the fusions will generate a term  $\partial_x \phi_\sigma$ . This leads to the following phenomenological expression for  $S^z(x)$ :

$$S^z(x) = -\frac{1}{\pi\sqrt{2}} \partial_x \phi_\sigma \sum_m A_{2m,z} \sin 2m(\sqrt{2}\phi_\rho - 2k_F x) + \sum_m A_{2m+1,z} \sin \sqrt{2}\phi_\sigma \sin(2m+1)(\sqrt{2}\phi_\rho - 2k_F x). \quad (108)$$

The usual expression of the spin density (20) is recovered for  $A_{2m,z} = 0$  and  $A_{2m+1,z} = 0$  for  $m \geq 1$ . For the  $S^{x,y}(x)$  similar expressions can be obtained. Starting from the phenomenological Haldane expansion of the fermion creation and annihilation operators [72]:

$$\psi_\sigma(x) \sim e^{\frac{i}{\sqrt{2}}(\theta_\rho + \sigma\theta_\sigma)} \sum_{m=-\infty}^{\infty} e^{i(2m+1)[\frac{(\phi_\rho + \sigma\phi_\sigma)}{\sqrt{2}} - k_F x]}, \quad (109)$$

we easily obtain:

$$S^+(x) \sim e^{i\sqrt{2}\theta_\sigma} \sum_{m,m'} e^{i[(m-m')(\sqrt{2}\phi_\rho - 2k_F x) + (m+m'+1)\sqrt{2}\phi_\sigma]}. \quad (110)$$

We note that  $m+m'+1$  and  $m-m'$  have different parities. We see easily that by fusion with  $\cos \sqrt{8}\phi_\sigma$ , the terms in  $\phi_\sigma$  with  $m+m'+1$  odd will be reduced to  $\cos \sqrt{2}\phi_\sigma$  while the terms with  $m+m'+1$  even will be reduced to 1. The expression of  $S^+(x)$  therefore reduces to:

$$S^+(x) \sim e^{i\sqrt{2}\theta_\sigma} \sum_m A_{2m+1,x} e^{i(2m+1)(\sqrt{2}\phi_\rho - 2k_F x)} + e^{i\sqrt{2}\theta_\sigma} \cos \sqrt{2}\phi_\sigma \sum_m A_{2m,x} e^{i2m(\sqrt{2}\phi_\rho - 2k_F x)}. \quad (111)$$

We can check that the expressions we have obtained lead to rotational invariant expression of the spin correlations for  $K_\sigma = 1$ , provided that  $A_{m,z} = A_{m,x}$  for all  $m$ .

Equations (108–111) can also be derived from a more physical argument. The Ogata-Shiba wavefunction tell us that in the limit of  $U/t \gg 1$ , the spin excitations can be described as a “squeezed” antiferromagnetic spin chains, the spins being carried by the electrons [58]. The spin density should therefore be described by the following expression:

$$\mathbf{S}(x) = \sum_n \mathbf{S}_n \delta(x - x_n), \quad (112)$$

where the  $x_i$  are the positions of the electrons along the chain, labelled in such way that  $x_1 < x_2 < \dots < x_N$ . The vector  $\mathbf{S}_n$  can be decomposed into a staggered and a uniform component as  $\mathbf{S}_n = \mathbf{J}_n + (-)^n \mathbf{n}_n$ . We will assume that both  $\mathbf{J}_n$  and  $\mathbf{n}_n$  are slowly varying at the scale of the average interparticle distance so that we can write:  $\mathbf{J}_n = \mathbf{J}(x = x_n)$ ,  $\mathbf{n}_n = \mathbf{n}(x = x_n)$ , the functions  $\mathbf{J}(x)$ ,  $\mathbf{n}(x)$  varying smoothly between the points  $x_n$ . We note that the integral from  $-\infty$  to  $+\infty$  of  $\mathbf{J}$  is the total magnetization operator and also the generator of the rotations. Thus, we expect the functions  $\mathbf{J}$  and  $\mathbf{n}$  to obey the following commutation relations:

$$[J^a(x), J^b(x')] = i\epsilon_{abc} J^c(x) \delta(x - x') (a \neq b), \quad (113)$$

$$[J^a(x), n^b(x')] = i\epsilon_{abc} n^c(x) \delta(x - x') (a \neq b), \quad (114)$$

that coincide with the usual commutation relation of the generator of the rotations and the staggered magnetic field [104]. Moreover, since the spin excitations of a spinful Luttinger liquid are expected to be described by a single

gapless boson, as those of a spin-1/2 chain, it is natural to identify  $\mathbf{J}$  to the bosonized uniform spin density of a spin 1/2 chain, and  $\mathbf{n}$  to the staggered spin density. The corresponding expression reads:

$$\begin{aligned} J^+(x) &= J^x + iJ^y \sim e^{i\sqrt{2}\theta_\sigma} \cos \sqrt{2}\phi_\sigma; n^+ \sim e^{i\sqrt{2}\theta_\sigma} \\ J^z &= -\frac{1}{\pi\sqrt{2}}\phi_\sigma; n^z \sim \sin \sqrt{2}\phi_\sigma. \end{aligned} \quad (115)$$

Let us now introduce a function  $\phi(x)$  such that  $\phi(x_n) = n\pi$ . We can rewrite the delta function as:

$$\begin{aligned} \sum_n \delta(x - x_n) &= \sum_n \delta(\phi(x) - n\pi) \frac{d\phi}{dx} \\ &= \sum_m e^{i2m\phi(x)} \frac{d\phi}{dx}, \end{aligned} \quad (116)$$

and we have:  $e^{i\phi(x)} = (-)^n$ . This allows us to write:

$$\mathcal{S}(x) = \mathbf{J}(x) \sum_m e^{i2m\phi(x)} \frac{d\phi}{dx} + \mathbf{n}(x) \sum_m e^{i(2m+1)\phi(x)} \frac{d\phi}{dx}. \quad (117)$$

Since  $\phi(x)$  must be  $n\pi$  each time that there is a particle, we have that  $\phi(x) = \phi_\uparrow(x) + \phi_\downarrow(x)$ , from which we easily obtain:  $\phi(x) = \pi\rho_0 x - \sqrt{2}\phi_\rho$ . Using the bosonized expressions (115) of  $\mathbf{J}$  and  $\mathbf{n}$  in terms of  $\phi_\sigma$  the expressions (108–111) are then easily seen to be equivalent to (117). Applying the expression (117) to our problem we see that the terms coming from the  $4k_F$  component of the spin density are less relevant and read:

$$(\cos 4\phi_{\rho+} + \cos 4\phi_{\rho-}) \mathbf{J}_1 \cdot \mathbf{J}_2. \quad (118)$$

The contribution of these terms to the Hamiltonian (22) can thus usually be neglected being less relevant. However, in the case of  $J_\perp$  sufficiently large, a gap may be formed in the modes  $\rho-, \sigma\pm$  at higher energy scale than in  $\rho+$ . In that case, the terms we have derived can lead to a modification of the coefficient  $g_0$  of the term  $\cos 4\phi_{\rho+}$  in (23) and a change of the ground state expectation value of  $\phi_{\rho+}$  from  $\frac{\pi}{4}$  to 0 if  $J_\perp$  is large enough.

## References

1. C. Chen, S. Cheong, Phys. Rev. Lett. **76**, 4042 (1996)
2. S. Mori, C. Chen, S. Cheong, Nature **392**, 473 (1998)
3. P. Monceau, F. Nad, S. Brazovskii, Phys. Rev. Lett. **86**, 4080 (2001)
4. J.M. Tranquada, D.J. Buttrey, V. Sachan, Phys. Rev. B **54**, 12318 (1996)
5. N. Ichikawa *et al.*, Phys. Rev. Lett. **85**, 1738 (2000)
6. E. Wigner, Trans. Faraday Soc. **34**, 678 (1938)
7. V.J. Emery, in *Highly Conducting One-Dimensional Solids*, edited by J.T. Devreese, R.P. Evrard, V.E. van Doren (Plenum Press, New York and London, 1979)
8. J. Sólyom, Adv. Phys. **28**, 209 (1979)
9. H.J. Schulz, in *Mesoscopic quantum physics, Les Houches LXI*, edited by E. Akkermans, G. Montambaux, J.L. Pichard, J. Zinn-Justin (Elsevier, Amsterdam, 1995), p. 533
10. S.R. White, Phys. Rev. Lett. **69**, 2863 (1992)
11. J. Hubbard, Phys. Rev. B **17**, 494 (1978)
12. H.J. Schulz, in “*Strongly correlated electronic materials*” *The Los Alamos symposium 1993*, edited by K.S. Bedell *et al.* (Addison-Westley, Reading, Massachusetts, 1994)
13. T. Giamarchi, Physica B **230-232**, 975 (1997)
14. M. Tsuchiizu, H. Yoshioka, Y. Suzumura, J. Phys. Soc. Jpn **70**, 1460 (2001)
15. D. Poilblanc, H. Tsunetsugu, T.M. Rice, Phys. Rev. B **50**, 6511 (1994)
16. S.R. White, D.J. Scalapino, Phys. Rev. Lett. **80**, 1272 (1998)
17. J. Bonca *et al.*, Phys. Rev. B **61**, 3261 (2000)
18. T. Tohyama *et al.*, Phys. Rev. B **59**, R11649 (1999)
19. S.R. White, I. Affleck, D.J. Scalapino, Phys. Rev. B **65**, 165122 (2002)
20. F.D.M. Haldane, Phys. Rev. Lett. **50**, 1153 (1983)
21. M. Takano *et al.*, Phys. Rev. Lett. **73**, 3463 (1994)
22. G. Chaboussant *et al.*, Phys. Rev. B **55**, 3046 (1997)
23. H. Iwase, M. Isobe, Y. Ueda, H. Yasuoka, J. Phys. Soc. Jpn **65**, 2397 (1996)
24. C. Rovira *et al.*, Angew. Chem. Inter. Ed. Engl. **36**, 2324 (1997)
25. B.C. Watson *et al.*, Phys. Rev. Lett. **86**, 5168 (2001)
26. C.P. Landee *et al.*, Phys. Rev. B **63**, 100402(R) (2001)
27. T. Rice, S. Gopalan, M. Sigrist, Europhys. Lett. **23**, 445 (1993)
28. M. Fabrizio, Phys. Rev. B **48**, 15838 (1993)
29. N. Nagaosa, Sol. State Comm. **94**, 495 (1995)
30. H.J. Schulz, Phys. Rev. B **53**, R2959 (1996)
31. L. Balents, M.P.A. Fisher, Phys. Rev. B **53**, 12133 (1996)
32. M. Fabrizio, A. Parola, E. Tosatti, Phys. Rev. B **46**, 3159 (1992)
33. D. Poilblanc, D.J. Scalapino, W. Hanke, Phys. Rev. B **52**, 6796 (1995)
34. M. Troyer, H. Tsunetsugu, T.M. Rice, Phys. Rev. B **53**, 251 (1996)
35. C.A. Hayward, D. Poilblanc, Phys. Rev. B **53**, 11721 (1996)
36. R. Noack, S. White, D. Scalapino, Phys. Rev. Lett. **73**, 882 (1994)
37. M. Uchara *et al.*, J. Phys. Soc. Jpn **65**, 2764 (1996)
38. M. Isobe, Y. Ueda, J. Phys. Soc. Jpn **65**, 1178 (1996)
39. A. Meetsma *et al.*, Acta Crystallogr. Sect. C **54**, 1558 (1998)
40. H. Smolinski *et al.*, Phys. Rev. Lett. **80**, 5164 (1998)
41. M. Mostovoy, D. Khomskii, Sol. State Comm. **113**, 159 (1999), cond-mat 9806215
42. H. Seo, H. Fukuyama, J. Phys. Soc. Jpn **67**, 2602 (1998)
43. T. Ohama, H. Yasuoka, M. Isobe, Y. Ueda, Phys. Rev. B **59**, 3299 (1999)
44. Y. Fagot-Revurat, M. Mehring, R.K. Kremer, Phys. Rev. Lett. **84**, 4176 (2000)
45. B. Grenier *et al.*, Phys. Rev. Lett. **86**, 5966 (2001)
46. H. Sawa *et al.*, J. Phys. Soc. Jpn **71**, 385 (2002)
47. M. Vojta, R.E. Hetzel, R.M. Noack, Phys. Rev. B **60**, R4817 (1999)
48. M. Vojta, A. Hubsch, R. Noack, Phys. Rev. B **63**, 045105 (2001)

49. H. Lin, L. Balents, M.P.A. Fisher, Phys. Rev. B **58**, 1794 (1998)
50. R. Konik, A.W.W. Ludwig, Phys. Rev. B **64**, 155112 (2001)
51. C. Wu, W.V. Liu, E. Fradkin, cond-mat/0206248 (unpublished)
52. M. Tsuchiizu, A. Furusaki, Phys. Rev. B **66**, 245106 (2002)
53. R. Amasaki, Y. Shibata, Y. Ohta, Phys. Rev. B **66**, 012502 (2002)
54. P. Horsch, F. Mack, Eur. Phys. J. B **5**, 367 (1998)
55. D. Sa, C. Gros, Eur. Phys. J. B **18**, 421 (2000)
56. S. Brazovskii, V. Yakovenko, J. Phys. Lett. France **46**, L111 (1985)
57. H. Tsunetsugu, M. Troyer, T.M. Rice, Phys. Rev. B **49**, 16078 (1994)
58. M. Ogata, H. Shiba, Phys. Rev. B **41**, 2326 (1990)
59. F.D.M. Haldane, Phys. Rev. Lett. **45**, 1358 (1980)
60. E. Jeckelmann, F. Gebhard, F.H.L. Essler, Phys. Rev. Lett. **85**, 3910 (2000)
61. D. Controzzi, F.H.L. Essler, A.M. Tsvelik, in *New Theoretical approaches to strongly correlated systems*, Vol. 23 of *NATO Science Series II. Mathematics, Physics and Chemistry*, edited by A.M. Tsvelik (Kluwer Academic Publishers, Dordrecht, 2001), p. 25
62. R. Shankar, Int. J. Mod. Phys. B **4**, 2371 (1990)
63. J.L. Black, V.J. Emery, Phys. Rev. B **23**, 429 (1981)
64. M.P.M. den Nijs, Phys. Rev. B **23**, 6111 (1981)
65. H.J. Schulz, Phys. Rev. Lett. **64**, 2831 (1990)
66. N. Kawakami, S.K. Yang, Phys. Rev. Lett. **65**, 2309 (1990)
67. N. Kawakami, S.K. Yang, Phys. Lett. A **148**, 359 (1990)
68. H. Frahm, V.E. Korepin, Phys. Rev. B **42**, 10553 (1990)
69. F. Mila, X. Zotos, Europhys. Lett. **24**, 133 (1993)
70. K. Sano, Y. Ōno, J. Phys. Soc. Jpn **63**, 1250 (1994)
71. M. Nakamura, K. Nomura, A. Kitazawa, Phys. Rev. Lett. **79**, 3214 (1997), cond-mat/9708204
72. F.D.M. Haldane, Phys. Rev. Lett. **47**, 1840 (1981)
73. H.J. Schulz, Phys. Rev. Lett. **71**, 1864 (1993)
74. D.V. Khveshenko, T.M. Rice, Phys. Rev. B **50**, 252 (1994)
75. M. Oshikawa, M. Yamanaka, I. Affleck, Phys. Rev. Lett. **78**, 1984 (1997)
76. J.L. Cardy, *Scaling and Renormalization in Statistical Physics, Cambridge Lecture Notes in Physics* (Cambridge University Press, Cambridge, UK, 1996)
77. J. Riera, D. Poilblanc, Phys. Rev. B **62**, R16243 (2000)
78. F.H.L. Essler, F. Gebhard, E. Jeckelmann, Phys. Rev. B **64**, 125119 (2001)
79. S.R. White, I. Affleck, Phys. Rev. B **54**, 9862 (1996)
80. D. Allen, D. Sénéchal, Phys. Rev. B **55**, 299 (1997)
81. D. Allen, F.H.L. Essler, A.A. Nersesyan, Phys. Rev. B **61**, 8871 (2000)
82. E. Witten, R. Shankar, Nucl. Phys. B **141**, 349 (1978)
83. O. Zachar, A.M. Tsvelik, Phys. Rev. B **63**, 033103 (2001), cond-mat/9909296
84. S. Fujimoto, N. Kawakami, J. Phys. Soc. Jpn **63**, 4322 (1994)
85. K. Le Hur, Phys. Rev. B **58**, 10261 (1998)
86. K. Le Hur, Phys. Rev. B **62**, 4408 (2000)
87. H. Schulz, cond-mat/9808167 (unpublished)
88. P. Azaria, A.O. Gogolin, P. Lecheminant, A.A. Nersesyan, Phys. Rev. Lett. **83**, 624 (1999)
89. D.G. Shelton, A.A. Nersesyan, A.M. Tsvelik, Phys. Rev. B **53**, 8521 (1996)
90. R. Assaraf, P. Azaria, M. Caffarel, P. Lecheminant, Phys. Rev. B **60**, 2299 (1999), cond-mat/9903057
91. P. Azaria, E. Boulat, P. Lecheminant, Phys. Rev. B **61**, 12112 (1999)
92. C. Itoi, S. Qin, I. Affleck, Phys. Rev. B **61**, 6747 (2000), cond-mat/9910109
93. S.K. Pati, R.R.P. Singh, D.I. Khomskii, Phys. Rev. Lett. **81**, 5406 (1998)
94. A. Nersesyan, A.M. Tsvelik, Phys. Rev. Lett. **78**, 3939 (1997), *ibid.*, **79**, E 1171
95. E. Orignac, R. Citro, N. Andrei, Phys. Rev. B **61**, 11533 (2000)
96. M. Fabrizio, A.O. Gogolin, A.A. Nersesyan, Nucl. Phys. B **580**, 647 (2000)
97. R. Shankar, Phys. Rev. Lett. **55**, 453 (1985)
98. Y.Y. Goldschmidt, Phys. Rev. Lett. **56**, 1627 (1986)
99. G.I. Japaridze, A.A. Nersesyan, JETP Lett. **27**, 334 (1978)
100. V.L. Pokrovsky, A.L. Talapov, Phys. Rev. Lett. **42**, 65 (1979)
101. H.J. Schulz, Phys. Rev. B **22**, 5274 (1980)
102. H.J. Schulz, Phys. Rev. B **59**, R2471 (1999)
103. R. Chitra, T. Giamarchi, Phys. Rev. B **55**, 5816 (1997)
104. I. Affleck, in *Fields, Strings and Critical Phenomena*, edited by E. Brezin, J. Zinn-Justin (Elsevier Science Publishers, Amsterdam, 1988)